

# Ancient TL

A periodical devoted to Luminescence and ESR dating

Institute of Geography and Earth Sciences, Aberystwyth University,  
Ceredigion SY23 3DB, United Kingdom

**Volume 30 No.1**

**June 2012**

**Introducing an R package for luminescence dating analysis**

S. Kreuzer, C. Schmidt, M.C. Fuchs, M. Dietze, M. Fischer and M. Fuchs \_\_\_\_\_ 1

**How many grains are there on a single aliquot?**

A.J. Heer, G. Adamiec and P. Moska \_\_\_\_\_ 9

**Towards a SAR-ITL protocol for the equivalent dose estimate of burnt quartzites**

C. Tribolo and N. Mercier \_\_\_\_\_ 17

**Thesis abstracts**

S. Vasiliniuc \_\_\_\_\_ 27

G. King \_\_\_\_\_ 28

J. Roskin \_\_\_\_\_ 28

G. Guérin \_\_\_\_\_ 30

**Bibliography** \_\_\_\_\_ 31

**Announcements**

UK Luminescence and ESR Meeting 2012, Aberystwyth \_\_\_\_\_ 39

ISSN 0735-1348

# Ancient TL

Started by the late David Zimmerman in 1977

---

## EDITOR

**G.A.T. Duller**, Institute of Geography and Earth Sciences, Aberystwyth University, Ceredigion SY23 3DB, United Kingdom ([ggd@aber.ac.uk](mailto:ggd@aber.ac.uk))

## EDITORIAL BOARD

**I.K. Bailiff**, Luminescence Dosimetry Laboratory, Dawson Building, University of Durham, South Road, Durham DH1 3LE, United Kingdom ([ian.bailiff@durham.ac.uk](mailto:ian.bailiff@durham.ac.uk))

**R.DeWitt**, Department of Physics, East Carolina University, Howell Science Complex, 1000 E. 5th Street Greenville, NC 27858, USA ([dewittr@ecu.edu](mailto:dewittr@ecu.edu))

**S.H. Li**, Department of Earth Sciences, The University of Hong Kong, Hong Kong, China ([shli@hku.hk](mailto:shli@hku.hk))

**R.G. Roberts**, School of Geosciences, University of Wollongong, Wollongong, NSW 2522, Australia ([rgrob@uow.edu.au](mailto:rgrob@uow.edu.au))

---

## REVIEWERS PANEL

**R.M. Bailey**, Oxford University Centre for the Environment, Dyson Perrins Building, South Parks Road, Oxford OX1 3QY, United Kingdom ([richard.bailey@ouce.ox.ac.uk](mailto:richard.bailey@ouce.ox.ac.uk))

**J. Faïn**, Laboratoire de Physique Corpusculaire, 63177 Aubièrre Cedex, France ([jean.fain@wanadoo.fr](mailto:jean.fain@wanadoo.fr))

**R. Grün**, Research School of Earth Sciences, Australian National University, Canberra ACT 0200, Australia ([rainer.grun@anu.edu.au](mailto:rainer.grun@anu.edu.au))

**T. Hashimoto**, Department of Chemistry, Faculty of Sciences, Niigata University, Niigata 950-21, Japan ([thashi@curie.sc.niigata-u.ac.jp](mailto:thashi@curie.sc.niigata-u.ac.jp))

**D.J. Huntley**, Department of Physics, Simon Fraser University, Burnaby B.C. V5A1S6, Canada ([huntley@sfu.ca](mailto:huntley@sfu.ca))

**M. Krbetschek**, Saxon Acad. of Sc., Quat. Geochron. Sect., Inst. Of Appl. Physics / TU Freiberg, Leipziger-Str. 23, D-09596 Freiberg, Germany ([quatmi@physik.tu-freiberg.de](mailto:quatmi@physik.tu-freiberg.de))

**M. Lamothe**, Dépt. Sci. de la Terre, Université du Québec à Montréal, CP 8888, H3C 3P8, Montréal, Québec, Canada ([lamothe.michel@uqam.ca](mailto:lamothe.michel@uqam.ca))

**N. Mercier**, Lab. Sci. du Climat et de l'Environ, CNRS-CEA, Av. de la Terrasse, 91198, Gif sur Yvette Cedex, France ([norbert.mercier@lscce.cnrs-gif.fr](mailto:norbert.mercier@lscce.cnrs-gif.fr))

**D. Miallier**, Laboratoire de Physique Corpusculaire, 63177 Aubièrre Cedex, France ([miallier@clermont.in2p3.fr](mailto:miallier@clermont.in2p3.fr))

**S.W.S. McKeever**, Department of Physics, Oklahoma State University, Stillwater Oklahoma 74078, U.S.A. ([stephen.mckeever@okstate.edu](mailto:stephen.mckeever@okstate.edu))

**A.S. Murray**, Nordic Laboratory for Luminescence Dating, Risø National Laboratory, Roskilde, DK-4000, Denmark ([andrew.murray@risoe.dk](mailto:andrew.murray@risoe.dk))

**N. Porat**, Geological Survey of Israel, 30 Malkhe Israel St., Jerusalem 95501, Israel ([naomi.porat@gsi.gov.il](mailto:naomi.porat@gsi.gov.il))

**D. Richter**, Lehrstuhl Geomorphologie, University of Bayreuth, 95440 Bayreuth, Germany ([daniel.richter@uni-bayreuth.de](mailto:daniel.richter@uni-bayreuth.de))

**D.C.W. Sanderson**, Scottish Universities Environmental Research Centre, Scottish Enterprise Technology Park, East Kilbride G75 0QF, UK ([David.Sanderson@glasgow.ac.uk](mailto:David.Sanderson@glasgow.ac.uk))

**A.K. Singhvi**, Rm 203, Physical Research Laboratory, Navrangpura, Ahmedabad 380009, India ([singhvi@prl.res.in](mailto:singhvi@prl.res.in))

**K.J. Thomsen**, Radiation Research Division, Risø National Laboratory for Sustainable Energy, Technical University of Denmark, DK-4000, Roskilde, Denmark ([krth@risoe.dtu.dk](mailto:krth@risoe.dtu.dk))

---

# Ancient TL

A periodical devoted to Luminescence and ESR dating

Web site: <http://www.aber.ac.uk/ancient-tl>

Institute of Geography and Earth Sciences  
Aberystwyth University SY23 3DB  
United Kingdom

Tel: (44) 1970 622606

Fax: (44) 1970 622659

E-mail: [ggd@aber.ac.uk](mailto:ggd@aber.ac.uk)



# Introducing an R package for luminescence dating analysis

Sebastian Kreutzer<sup>1,2\*</sup>, Christoph Schmidt<sup>3</sup>, Margret C. Fuchs<sup>4</sup>, Michael Dietze<sup>5</sup>, Manfred Fischer<sup>2</sup> and Markus Fuchs<sup>1</sup>

<sup>1</sup>Department of Geography, Justus-Liebig-University Giessen, 35390 Giessen, Germany

<sup>2</sup>Geographical Institute, Geomorphology, University of Bayreuth, 95440 Bayreuth, Germany

<sup>3</sup>Institute for Geography, University of Cologne, 50923 Cologne, Germany

<sup>4</sup>Department of Geology, TU Bergakademie Freiberg, 09599 Freiberg, Germany

<sup>5</sup>Institute of Geography, TU Dresden, 01069 Dresden, Germany

\* corresponding author: [sebastian.kreutzer@geogr.uni-giessen.de](mailto:sebastian.kreutzer@geogr.uni-giessen.de)

(Received 16 May 2012; in final form 27 May 2012)

## Abstract

For routine luminescence dating applications the commonly used Risø readers are bundled with analysis software, such as *Viewer* or *Analyst*. These software solutions are appropriate for most of the regular dating and publication jobs, and enable assessment of luminescence characteristics and provide basic statistical data treatment. However, for further statistical analysis and data treatments, this software may reach its limits. In such cases, open programming languages are a more appropriate approach. Here, we present the **R** package ‘Luminescence’ for a more flexible handling of luminescence data and related plotting purposes, using the statistical programming language **R**. The **R** language as well as the package and the source code are provided under the General Public License (GPL) conditions and are available for free. The basic functionality of the package is described along with three application examples. This package is not an alternative to the existing software (*Analyst*, *Viewer*) but may provide a collection of additional tools to analyse luminescence data and serve as a platform for further contributions.

**Keywords:** R, luminescence dating, LM-OSL, curve fitting, radial plot

## Introduction

Since the early beginnings of luminescence dating at the end of the 1950s (Daniels et al. 1953, Houtermans and Stauffer 1957, Grögler et al. 1958), the method of luminescence dating has advanced considerably. Not least, a widespread application in geosciences has become possible with the development of commercially available, computerised and automatic measurement equipment (e.g. Risø, Daybreak, Freiberg Instruments) and reliable measurement protocols (e.g. single aliquot

regenerative (SAR) protocol by Murray and Wintle 2000). For the analysis of measured data in routine luminescence dating applications, the commonly used Risø reader is bundled with software such as the *Viewer* or *Analyst* (Duller 2007). Considering the analysis, export and graphical output functions, this software is sufficient for most of the everyday dating and publication purposes. However, experimental and exploratory luminescence studies require more computational flexibility and further statistical data treatment. In addition, more recent methods such as the linearly modulated luminescence analysis (Bulur 1996) ask for a more comprehensive analysis software. Furthermore, compiled and ready to use software solutions are black boxes to non-software engineers, even if the source code is provided. Our attempts to find an easy-to-use and scalable numerical computational environment, able to 1) import OSL measurement data, 2) process the imported data with a modular, extendable toolbox of readily available and open source functions and 3) generate high-quality numerical and graphical output was met by the statistical software **R** (R Development Core Team 2012).

The **R** programming environment was introduced in 1996 by Ihaka and Gentleman (1996) and is based on the **S** system/language developed by John Chambers (e.g. Hornik and Leisch 2002). Scripts written in **R** are in general compatible to the commercially available implementation of the **S** system called ‘S-PLUS’ (e.g. Hornik and Leisch 2002, Ligges 2008). The main advantages of using **R** are: (1) The **R** language is intuitive and easy to learn, (2) **R** is open source software and therefore free of charge, (3) a growing community offers a fast and high-quality support, (4) **R** is available for all major computer platforms and the language itself is almost independent of the operating system, (5) **R** is modular and highly extensible through user defined

**Table 1:** Functions in the **R** package ‘Luminescence’ (vers. 0.1.7)

Name	Description
Analyse_SAR.OSLdata()	Analyse SAR CW-OSL measurements
Calc_FadingCorr()	Applying a fading correction according to Huntley and Lamothe (2001) for a given age and a given g-value
Calc_FuchsLang2001()	Calculate $D_e$ applying the method of Fuchs and Lang (2001)
Calc_OSLLxTxRatio()	Calculate $L_x/T_x$ ratio for a given set of OSL curves
CW2pLM()	Transform a CW-OSL curve into a pseudo-LM (pLM) curve (e.g. Bulur, 2000)
fit_LMCurve()	Non-linear Least Squares (NLS) fit for LM-OSL curves
plot_BINfileData()	Plot single luminescence curves from a BIN-file object (readBIN2R())
plot_DeDistribution()	Plot $D_e$ distribution with a kernel density estimate (KDE)
plot_GrowthCurve()	Fit and plot a growth curve for luminescence data
plot_Histogram()	Plot a histogram with a separate error plot
plot_RadialPlot()	Plot a Galbraith's radial plot
readBIN2R()	Import Risø BIN-file into <b>R</b>
Second2Gray()	Converting values from seconds (s) to Gray (Gy)

packages. Especially the latter advantage points to the great potential in terms of experimental and increasingly wide application of luminescence investigations and is therefore the motivation for our contribution. Additionally, (6) already existing statistical tools of data analysis (e.g. the minimum age model of Galbraith et al. 1999) can directly be applied or implemented using the same software: **R**.

In general, **R** can be described as software for statistical computing by default without a graphical user interface but with a command line or terminal. It provides a powerful tool, once the **R** language has been assimilated. Our first **R** scripts were written to produce plots from \*.csv (comma separated values) files, e.g. probability density plots, or to calculate statistical parameters from extensive data sets. However, when sharing the scripts with a growing community, the consequence is to encapsulate the **R** code into functions and bundle them within a separate **R** package. A package can be installed and loaded into the **R** environment. The provided functions work as small applications within the **R** environment while the source code of the scripts is always available and the calculations are therefore transparent for the user. Along with the **R** code itself, a documentation file for every function is available as well as additional example data, which have been thoroughly tested in advance.

Here we present the **R** package ‘Luminescence’ in its latest version (0.1.7) including a set of functions for data import, analysis of luminescence properties, statistical data processing and result plotting, e.g.  $D_e$  distributions, growth curves or calculate  $L_x/T_x$  values for a given set of curves (Table 1). The basic features are presented using three examples of typical

applications: (1) Importing BIN-files, (2) plotting  $D_e$  distributions, (3) fitting LM-OSL curves. Along with these functions, example data sets are delivered. Nevertheless, this paper is not an introduction to the **R** language nor is it possible to present all functions bundled within the package in detail. We tried to keep all examples as simple as possible. The given **R** code is intended to: (1) provide a short insight into how **R** and the package work (for readers who are not familiar with the **R** language) and (2) allow **R** users to roughly assess the basic functionality of the package.

### Examples

To provide an overview of the basic functionality we focus on three application examples. For further functions the reader is referred to the manual of the package. The chosen examples are given as **R** code with the corresponding (reduced) terminal output. Code, terminal output and **R**-relating functions are indicated by monospaced letters. All examples were produced using the freely available integrated development environment (IDE) *RStudio™ Desktop* (<http://rstudio.org>) but the reader may also use other **R** IDEs or the **R** terminal.

#### Example 1: Importing \*.bin files

A crucial question for data analysis usually is how to import the measured data to the preferred software. Substantial time is often spent before starting the data analysis undertaking data transformation and format conversion. The measurement results of the Risø readers are stored in a binary file format (\*.bin, BIN-file) containing various data of the measurements. There are several ways to export

binary measurement data to more general exchange formats such as the ASCII format. The *Analyst* software as well as the *Risø Viewer* offers export functionalities of the raw data into an ASCII file. An alternative is the *MS Windows<sup>TM</sup>* terminal program ‘*Bin2Ascii*’ written in C (Bailey 2008). It produces separate ASCII files for every measured curve in one run. Furthermore, there may be numerous individual software solutions, written and used by various researchers throughout the luminescence community. In general, at least one additional step is needed to import the measured data into R but the metadata stored in the BIN-file (e.g. read temperature, type of stimulation) may get lost for further usage. However, the format of the BIN-file is described in detail in the *Analyst* manual (Duller 2007) which allowed us to develop an R function that directly imports the entire BIN-file into the R environment to maintain all provided data. The corresponding function is called `readBIN2R()` and has been successfully tested for BIN-files produced by the *Sequence Editor* of version 3.x and 4.x. To import a BIN-file into the R environment the function requires one argument containing the path and the name of the BIN-file:

```
> temp<-readBIN2R("~/Desktop/test.BIN")
> temp
Risoe.BINfileData Object
  Version:      03
  Object Date:  270520
  User:        x
  System ID:    0
  Overall Records: 1104
  Records Type: OSL=720;TL=336;IRSL=48;
  Position Range: 1 : 48
  Run Range:    1 : 45
  Set Range:    1 : 16
```

The `readBIN2R()` function returns an R object with two slots: `@METADATA` and `@DATA`. The first one is a `data.frame` object containing the metadata of the measurement as shown in the *Analyst*, the second slot contains a `list` object containing vectors with the measured count data.

```
> temp@METADATA[1:2,1:6]
  ID SEL VERSION LENGTH PREVIOUS NPOINTS
1  TRUE  03   672      0      100
2  TRUE  03   672     672     100

> unlist(temp@DATA[1])[1:10]
[1] 140 138 133 143 129 123 134 134 129 143
```

The provided metadata equals what is shown when using the ‘Display Information’ options in the *Analyst*. The metadata can be used to select certain curve data for further analysis. For example, to select the record IDs (which are identical to the IDs in the

slot `@DATA`) of all measured OSL data from the measurement, in R the following code is required:

```
> temp@DATA[temp@METADATA[temp@METADATA[,
+"LTYPE"]== "OSL", "ID"]]
```

Note: Working with the package does not mean that the input data has to be a BIN-file. For other formats, e.g. \*.csv or \*.txt, R provides generic functions that can be used instead (e.g. `read.csv()` or `read.table()`).

### Example 2: Plotting $D_e$ distributions

The next example was chosen to focus on what is of most general relevance and an essential advantage of R, the production of high-quality plots in different file formats. Creating figures for publication or presentation might be a time consuming and sometimes frustrating process. Once the plotting functions for a desired figure design have been created in R, the code can be reused almost universally with only minor modifications (e.g. modifying the input arguments). In the package we bundled a few plot functions, which produce plots that are commonly used to present luminescence dating results. Here we focus on two frequently used plot alternatives: (1) empirical cumulative distribution along with kernel density estimates (KDE) and (2) the radial plot. Within the package the function to produce an empirical distribution along with the KDE is called `plot_DeDistribution()` and the radial plot function `plot_RadialPlot()`. Both require as input a two column `data.frame` containing x-y-values (e.g.  $D_e$  and  $D_e$  error). Here a fine grain quartz loess sample from Saxony/Germany (BT998, unpublished data) is used as an example data set:

```
> ExampleData.DeValues[1:3,]
      x      y
1 207.5040 7.3062
2 208.3326 7.0470
3 227.1216 9.3216
```

The plot output (Figure 1) gives the  $D_e$  values with their corresponding  $D_e$  error in ascending order and additionally shows the basic  $D_e$  distribution parameters (number of  $D_e$ , mean, standard deviation). The KDE is shown as a blue line. It is produced with:

```
> plot_DeDistribution(ExampleData.DeValues)
```

For plotting a radial plot (e.g. Galbraith 1988) on a log z-scale the R code is quite similar:

```
> plot_RadialPlot(ExampleData.DeValues)
```

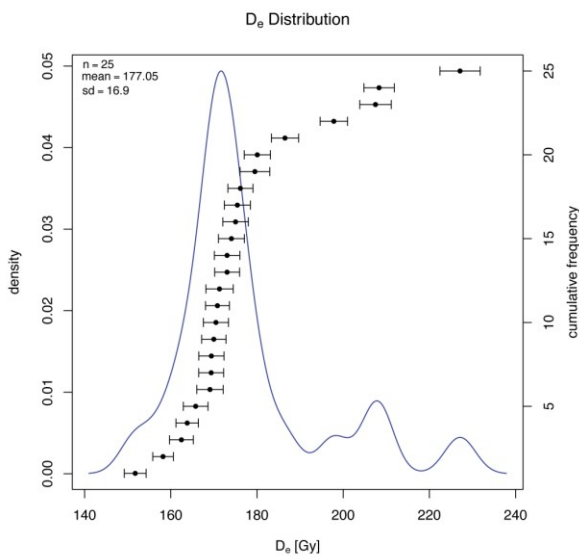


**Figure 1:**  $D_e$  distribution with kernel density plot for a fine grain quartz sample (BT998). Plot output for the function `plot_DeDistribution()`, the aliquots are shown in ascending  $D_e$  order. Note: the function does not check if the input values are given in e.g. Gray or seconds, or if the given values are  $D_e$  values or not.

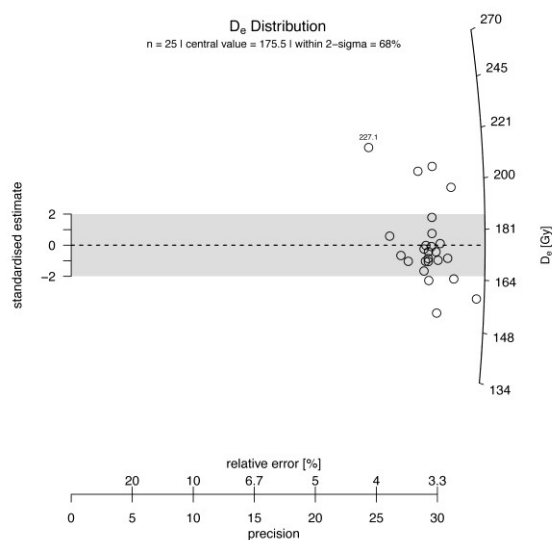


**Figure 2:**  $D_e$  distribution shown as a radial plot for a fine grain quartz sample (BT998) as output of the function `plot_RadialPlot()`. The numeric value within the plot indicates the highest  $D_e$  value.

The resulting radial plot is shown in Figure 2. The function is based on an **S** script of Rex Galbraith, but has been rewritten to reduce the needed manual adjustments.

Using generic functions of **R**, the plot can be further exported into several formats (e.g. JPEG, SVG, PDF). For the given function an export as PDF requires just a minor extension, e.g. by stating the desired file format with the arguments of output path and plot size:

```
> pdf("~/Desktop/Figure1.pdf", paper=
+ "special")
+ plot_DeDistribution(ExampleData.DeValues,
+ xlab="s")
+ dev.off()
```

For a more general discussion of the advantages and disadvantages of the different plot types the reader is referred to Galbraith and Roberts (in press).

### Example 3: LM-OSL curve fitting

Since the introduction of optically stimulated luminescence (OSL) dating by Huntley et al. (1985), it has been reported that the continuous wave (CW) OSL signals from quartz decay non-exponentially. Bailey et al. (1997) postulated that the quartz signal consists of, at least, three distinct components (termed as fast, medium and slow) with different bleaching and dose-response characteristics. In 1996, Bulur (1996) presented an alternative read-out method by ramping the stimulation intensity over time, termed the linear modulation technique (LMT or LM-OSL). The obtained peak-shaped curve is supposed to be associated with the successive release of electrons from traps/components with increasing optical stability (i.e. decreasing detrapping probability) during measurement (e.g. Bulur 2000).

As a result of the different and sometimes disadvantageous component characteristics (e.g. bleachability, thermal stability), for routine quartz sediment dating the underlying assumption is that the chosen integral of the bulk luminescence signal is dominated by an easy-to-bleach signal component and the contribution of other components can be minimised, e.g. by early background subtraction (Ballarini et al. 2007). Another approach is the isolation of the fast-component by direct measurement (Bailey 2010) or decomposition of the signal by mathematical curve fitting (CW- or LM-OSL curve fitting).

Besides the discussion of the difficulties resulting from the mathematical fitting itself (e.g. Istratov and Vyvenko 1999, Bailey 2010, Bailey et al. 2011), the limitation of this method for routine applications seems to be more of a practical nature. The decomposition of a single LM-OSL curve usually involves a multistep process using different

programs. Therefore, attempting to fit multiple curves is a time consuming process. During the last years a few attempts were presented based on proprietary or self-written software (e.g. Singarayer 2002, Choi et al. 2006, Bailey 2008) to fit LM-OSL curves or CW-OSL curves (e.g. Rowan et al. 2012). To offer an alternative, and to fit a batch of curves automatically, we decided to implement a fitting routine, making the fitting process much more flexible in the way the background is subtracted or the plot output is produced. This approach is transparent and applicable for extensive data sets and further analysis. To avoid any confusion: We did not develop a new mathematical fitting algorithm, but rather used the implemented functions of **R** to write a new function (`fit_LMData()`) that covers the needs in the context of OSL dating of quartz with references to the cited literature. Therefore, we employed the internal non-linear least-square fitting function `nls()` with the `port` algorithm (<http://www.netlib.org/port/>) and the 1<sup>st</sup> order kinetic function given by Kitis and Pagonis (2008). More information is provided on the help pages of the package. As input file, at least one `data.frame` containing LM-curve data (measured data) with two columns (time, counts) is required:

```
> values.curve
      time counts
1      1     48
2      2     19
3      3     23
.      .      .
.      .      .
4000 4000    530
```

The values from an LM-OSL measurement of a coarse grain (90 – 250  $\mu\text{m}$ ) quartz sample from Norway (BT900, Fuchs et al. in press) are shown. To run a fit to the `data.frame` (`values.curve`) trying a 3-component function on a log-time scale (x-axis) the code in **R** is:

```
> fit_LMCurve(values=values.curve,n.
+ components=3,log_scale="x")
```

The resulting plot for sample BT900 is shown in Figure 3. If an additional curve for the measured background (2<sup>nd</sup> LM-curve) is provided as a two column `data.frame`, here termed as `values.curveBG`, the background is fitted using a polynomial function and subtracted automatically from the first curve. The result is shown in Figure 4, and the corresponding call in **R** is:

```
>fit_LMCurve(values=values.curve, values.bg=
+ values.curveBG,+n.components=3,
+ log_scale="x", output.plotBG=TRUE)
```

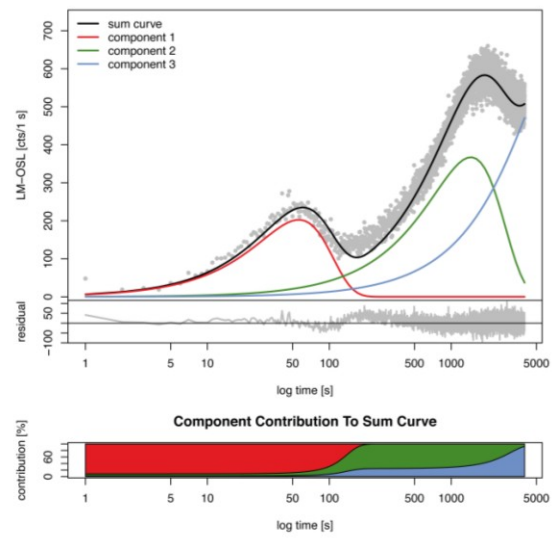


**Figure 3:** LM-OSL curve from a coarse grain quartz sample (BT900) fitted with a 3-component function plotted using the function `plot_LMCurve()` without background subtraction. The lower plot shows the contribution of each component to the light sum.

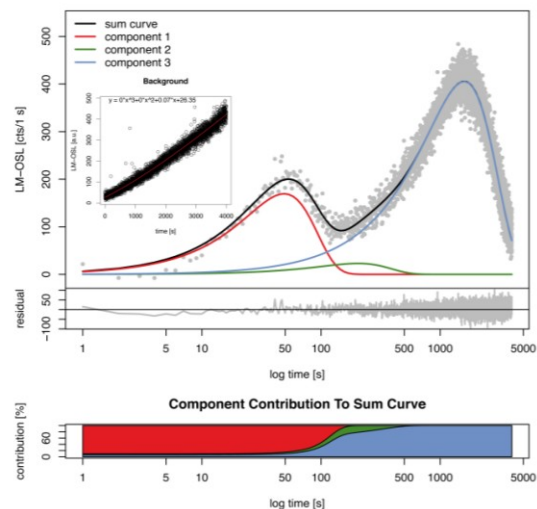


**Figure 4:** LM-OSL curve from a coarse grain quartz sample (BT900) fitted with a 3-component function using the function `plot_LMCurve()` including background subtraction. The lower plot shows the contribution of each component to the light sum. The fitted background signal (separate curve) is shown in the inset.

Along with the optional plot and terminal output (not shown) a `nls()` object is returned. This **R** object contains all data from the fit (e.g. parameters,

residuals) and can be used for further analysis using generic functions of **R**, e.g. calculating confidence intervals for the fitted parameters (`confint()`). The start parameters for the fitting are estimated automatically, but also manual start parameters will be accepted. With this, for instance, the function can be used in a loop to test different sets of start parameters and compare them with the obtained quality of the fit (i.e. pseudo- $R^2$ ) or to fit many curves in one run. An example for a fitting loop over all LM-curves of a measurement is given in the supplementary data.

To compare the results with other software solutions (obtained  $b_i$  and  $n_i$  values for a given number of components), we conducted a survey comparing the results from this **R** package with results returned by the software from Diana Bailey (FitBin9, Bailey 2008) and Grzegorz Adamiec (Hybfit, principle described in Bluszcz and Adamiec 2006). Three different samples (Supplementary Table 1) were used for this study: (a) a sample from a beach deposit in Norway (BT900, Fuchs et al. in press), (b) a Mol-sand sample from Belgium (MOL1, Gullentops and Vandenberghe 1995) and (c) an archaeological artefact (chalcedony) from Romania (Rom16, Schmidt et al., in prep.). The LM-OSL curves of the samples were fitted with and without background subtraction using the automatic start parameter recognition option of the software for a given number of components. For the investigated LM-OSL curves without background subtraction we observed that the shapes of the curves were indistinguishable. The use of the software's background subtraction option results in differences in the fitting parameters, probably due to the way of background subtraction (Supplementary Table 2). However, if no background subtraction is applied, the output of the software visually appears to be very similar. A typical LM fit for sample BT900 is shown in Figure 5. Detailed results of the comparison are given in the supplementary.

## Discussion

This paper briefly describes an **R** package for luminescence dating and reports the advantages compared to existing software. The **R** programming language, although intuitive to users having basic knowledge in numerical programming languages (e.g. *MATLAB*<sup>TM</sup> or *Mathematica*<sup>TM</sup>), is not as user friendly as the *Analyst*, the *Risø Viewer*, *MS Excel*<sup>TM</sup> or *SigmaPlot*<sup>TM</sup>. However such a comparison would be misleading. **R** allows the creation of complex and transparent data analysis routines for experimental protocols that are not available in existing software. The presented package is not standalone software and is not intended to be such. The presented package provides a collection of functions, serving as a

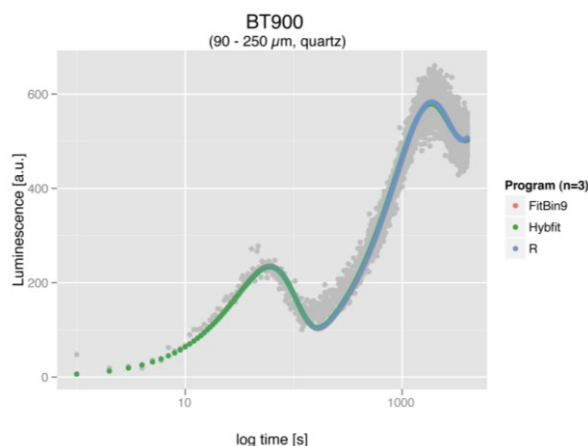


**Figure 5:** LM-OSL fitting using a 3-component function for the quartz sample BT900 on a log scale. The sum curves show that all programs produce similar fits and therefore the three curves are indistinguishable.

flexible, modular and easy to extend toolbox for the purpose of luminescence dating with special focus on the analysis of non-standardised measurements. The comparison of the fitting programs (**R**, FitBin9 and Hybfit) showed that by default **R** is bundled with powerful libraries and functions like the used `nls()` function producing reliable fitting results. Nevertheless, this is no out-of-the box tool and has to be adjusted for the purpose of luminescence dating. In contrast, using the *Analyst* software is a straightforward process for routine luminescence data analysis and therefore every day in use in our laboratories.

In summary, our contribution is intended to point to the possibilities provided by **R**, the existence of the 'Luminescence' package and to invite other **R** users to contribute and further improve the package. Not least our work may encourage others to start working with **R**.

## Conclusions

An **R** package ('Luminescence') for luminescence dating data analysis has been presented and the basic features were shown by three examples. The **R** package is provided under the General Public Licence (GPL)<sup>1</sup> conditions and is available for free. The package in its latest version including the manual is distributed over the Comprehensive **R** Archive Network (CRAN)<sup>2</sup>.

The reader may also have noticed that in the luminescence dating community several **R/S** scripts

<sup>1</sup> <http://www.gnu.org/licenses/gpl-3.0.html>

<sup>2</sup> <http://cran.r-project.org/web/packages/Luminescence/index.html>

(e.g. from Rex Galbraith or Lee Arnold) are circulating. These scripts are not (yet) part of the presented **R** package. Furthermore, herewith we invite everyone to contribute to the package.

### Acknowledgments

We are thankful to Rex Galbraith for his permission to publish the radial plot function under GPL and his useful comments on the rewritten plot function. Grzegorz Adamiec is thanked for helpful discussions on the fitting procedure using the program Hybfit. We are furthermore thankful to Diana Bailey for providing the fitting program FitBin9 for the comparison of the programs. The work of the corresponding author was gratefully funded by the DFG (FU 417/7-2).

### Supplementary Information

Supplementary Information for this article can be found at [www.aber.ac.uk/ancient-tl](http://www.aber.ac.uk/ancient-tl)

### References

- Bailey, D.J.E. (2008). Development of LM OSL analysis techniques for applications to optical dating. Unpublished DPhil thesis, University of Oxford.
- Bailey, R.M. (2010). Direct measurement of the fast component of quartz optically stimulated luminescence and implications for the accuracy of optical dating. *Quaternary Geochronology*, **5**, 559–568.
- Bailey, R.M., Smith, B.W., Rhodes, E.J. (1997). Partial bleaching and the decay form characteristics of quartz OSL. *Radiation Measurements*, **27**, 123–136.
- Bailey, R.M., Yukihara, E.G., McKeever, S.W.S. (2011). Separation of quartz optically stimulated luminescence components using green (525 nm) stimulation. *Radiation Measurements*, **46**, 643–648.
- Ballarini, M., Wallinga, J., Wintle, A.G., Bos, A.J.J. (2007). A modified SAR protocol for optical dating of individual grains from young quartz samples. *Radiation Measurements*, **42**, 360–369.
- Bluszcz, A., Adamiec, G. (2006). Application of differential evolution to fitting OSL decay curves. *Radiation Measurements*, **41**, 886–891.
- Bulur, E. (1996). An alternative technique for optically stimulated luminescence (OSL) experiment. *Radiation Measurements*, **26** (5), 701–709.
- Bulur, E. (2000). A simple transformation for converting CW-OSL curves to LM-OSL curves. *Radiation Measurements*, **32**, 141–145.
- Choi, J.H., Duller, G.A.T., Wintle, A.G. (2006). Analysis of quartz LM-OSL curves. *Ancient TL*, **24**, 9–20.
- Daniels, F., Boyd, C.A., Saunders, D.F. (1953). Thermoluminescence as a Research Tool. *Science*, **117** (3040), 343–349.
- Duller, G.A.T. (2007). *Analyst. Manual*, 1–45.
- Fuchs, M., Kreutzer, S., Fischer, M., Sauer, D., Sørensen, R. (in press). OSL and IRSL dating of raised beach sand deposits along the southeastern coast of Norway. *Quaternary Geochronology*, doi:10.1016/j.quageo.2011.11.009.
- Fuchs, M., Lang, A. (2001). OSL dating of coarse-grain fluvial quartz using single-aliquot protocols on sediments from NE Peloponnese, Greece. *Quaternary Science Reviews*, **20**, 783–787.
- Galbraith, R.F. (1988). Graphical display of estimates having differing standard errors. *Technometrics*, **30**, 271–281.
- Galbraith, R. F., Roberts, R. G., Laslett, G. M., Yoshida, H., Olley, J. M. (1999). Optical dating of single and multiple grains of Quartz from Jinnium Rock Shelter, Northern Australia: Part I, Experimental design and statistical models, *Archaeometry*, **41**, 339–364.
- Galbraith, R. F., Roberts, R. G. (in press). Statistical aspects of equivalent dose and error calculation and display in OSL dating: An overview and some recommendations, *Quaternary Geochronology* doi:10.1016/j.quageo.2012.04.020.
- Grögler, N., Houtermans, F.G., Stauffer, H. (1958). Radiation damage as a research tool for geology and prehistory. 5<sup>o</sup> Rassegna Internazionale Elettronica E Nucleare, Supplemento Agli Atti Del Congresso Scientifico, **1**, 5–15.
- Gullentops, F., Vandenberghe, N. (1995). Toelichtingen Bij De Geologische Kaart Van Belgie Vlaams Gewest: Kaartblad 17 Mol. 1–66.
- Hornik, K., Leisch, F. (2002). Vienna and R: Love, marriage and the future. *Festschrift - 50 Jahre Österreichische Statistische Gesellschaft*, 61–20.
- Houtermans, F.G., Stauffer, H. (1957). Thermolumineszenz als mittel zur Untersuchung der Temperatur - und Strahlungsgeschichte von Mineralien und Gesteinen. *Helvetica Physica Acta*, **30**, 274–277.
- Huntley, D.J., Godfrey-Smith, D.I., Thewalt, M.L.W. (1985). Optical dating of sediments. *Nature*, **313**, 105–107.
- Huntley, D.J., Lamothe, M. (2001). Ubiquity of anomalous fading in K-feldspars and the measurement and correction for it in optical dating. *Canadian Journal of Earth Sciences*, **38**, 1093–1106.
- Ihaka, R., Gentleman, R. (1996). R: A Language for Data Analysis and Graphics. *J. Computational and Graphical Statistics*, **5**, 299–314.

- Istratov, A.A., Vyvenko, O.F. (1999). Exponential analysis in physical phenomena. *Review of Scientific Instruments*, **70**, 1233–1257.
- Kitis, G., Pagonis, V. (2008). Computerized curve deconvolution analysis for LM-OSL. *Radiation Measurements*, **43**, 737–741.
- Ligges, U. (2008). Programmieren mit R (Statistik und ihre Anwendungen). Springer.
- Murray, A.S., Wintle, A.G. (2000). Luminescence dating of quartz using an improved single-aliquot regenerative-dose protocol. *Radiation Measurements*, **32**, 57–73.
- R Development Core Team (2012). R: A Language and Environment for Statistical Computing. R Foundation for Statistical Computing, <http://www.R-project.org/>.
- Rowan, A.V., Roberts, H.M., Jones, M. A., Duller, G.A.T., Covey-Crump, S.J., Brocklehurst, S.H. (2012). Optically stimulated luminescence dating of glaciofluvial sediments on the Canterbury Plains, South Island, New Zealand, *Quaternary Geochronology*, **8**, 10-22.
- Schmidt, C., Sitlivy, V., Anghelinu, M., Chabai, V., Kels, H., Uthmeier, T., Hauck, T., Bălcean, I., Hilgers, A., Richter, J., Radtke, U. (in prep). Unexpectedly old: thermo-luminescence dating of heated artefacts from the Aurignacian open-air site of Românești-Dumbrăvița I, Romania.
- Singarayer, J.S. (2002). Linearly modulated optically stimulated luminescence of sedimentary quartz: physical mechanisms and implications for dating. Unpublished DPhil thesis, University of Oxford.

#### Reviewer

G.A.T. Duller

#### Reviewers Comments

R is increasingly being used for a wide range of scientific applications, both in Earth and Physical Sciences. This excellent package is a very welcome contribution and I hope that it will encourage many luminescence colleagues to explore the use of this powerful software.

The authors have also provided a very valuable help file as part of the Luminescence Package, and this can be accessed from within **R** by typing:

```
help(Luminescence)
```

# How many grains are there on a single aliquot?

Aleksandra J. Heer<sup>1\*</sup>, Grzegorz Adamiec<sup>2\*</sup> and Piotr Moska<sup>2</sup>

<sup>1</sup>Institute of Geography, University of Bern, Hallerstrasse 12, 3012 Bern, Switzerland

<sup>2</sup>Department of Radioisotopes, Institute of Physics, Silesian University of Technology, ul. Krzywoustego 2, 44-100 Gliwice, Poland

\*corresponding authors AJH: [heer@giub.unibe.ch](mailto:heer@giub.unibe.ch); GA: [grzegorz.adamiec@polsl.pl](mailto:grzegorz.adamiec@polsl.pl)

(Received 23 April 2012; in final form 25 May 2012)

## Introduction

In our recent OSL studies on modelling equivalent doses ( $D_e$ ) obtained using single aliquots the question arose how many grains are present on a single aliquot and consequently, how many grains on a single aliquot contribute to the measured signal?

To date, the usual practice reported in literature has been to calculate the maximum number of grains predicted on the basis of dense packing of circles on a plane assuming an average diameter of the hypothetically spherical grains (e.g. Rhodes 2007, Duller 2008, Arnold and Roberts 2009). When grains are attached to the disc surface through a medium like silicone oil sprayed on a disc through a circular mask, the number of grains is estimated from the size of the total area covered by grains and the surface area of the cross section of the spherical grain. So for example a 4 mm diameter aliquot of 90-125  $\mu\text{m}$  diameter spherical grains would consist of a maximum number of grains ( $n$ ):

$$n = \frac{\pi \cdot 2^2}{\pi \cdot 0.0538^2} \cdot \frac{\pi}{\sqrt{12}} \approx 1253 \text{ grains}$$

calculated for the middle of the diameter range, where  $\frac{\pi}{\sqrt{12}}$  is the densest packing factor of a plane

by circles of equal diameters in hexagonal arrangement, first given by Lagrange. A 6 mm diameter aliquot of 200-250  $\mu\text{m}$  diameter grains would contain a maximum of:

$$n = \frac{\pi \cdot 3^2}{\pi \cdot 0.113^2} \cdot \frac{\pi}{\sqrt{12}} \approx 639 \text{ grains}$$

In general, grains are not spherical, their size varies, and the packing is unlikely to be perfect. These factors influence the number of grains present on a disc. In this communication we report our investigations of the number of grains present on a single aliquot of sedimentary quartz.

## Experimental

The number of grains on an aliquot was determined for aliquots prepared using the standard method applied in the Bern OSL laboratory.

The discs are placed in a holder and after covering the holder with a mask with circular holes located at the centres of discs, the discs are sprayed with silicone oil. The oil circles have the desired diameter of the aliquot. Subsequently, the grains are placed on a sheet of paper and the discs held by tweezers are pressed on the grains with the side with the attached silicone oil. After that, the discs are tapped on their sides to remove the excess of grains to ensure that grains form a monolayer.

In the current study we used a mask with 6 mm diameter holes. In order to count the number of grains, we took photos of the aliquots using a Leica M 205C binocular microscope equipped with a digital camera Leica DFC 280. The photos were taken at a magnification of 12.5x, printed on A4 format and manually counted.

The quartz studied originated from NW alpine postglacial sediments from the profile Mattenhof located at Wauwilermoos on the Swiss Plateau. The 200-250  $\mu\text{m}$  diameter grains were from the sample WAU-MH3 and grains 150-200  $\mu\text{m}$  in diameter were from the sample WAU-MH2.

## Results

The photographs (examples are shown in Figure 1) reveal that the quartz grains in these samples are only slightly rounded, mainly sharp-edged and the grains are of cubic, cuboid or elongated, thin and point-tapered shapes (Figure 1a). The heterogeneity of shapes may be the result of the rather short sedimentary history and limited mechanical abrasion by the glacier. It appears that within the 6 mm circle there is considerable space free of grains, contrary to the usual assumption of dense coverage by grains (Figure 1b).

**Table 1:** Results of counting grains on single aliquot discs.

Grain size	Aliquot diameter (mm)	Number of counted aliquots	Calculated <sup>1)</sup> maximum number of grains	Counted average number of grains	Standard deviation	Packing ratio (%)
150-200 $\mu\text{m}$	6	46	1073	677	48	63
200-250 $\mu\text{m}$		52	634	440	46	65

<sup>1)</sup> a monolayer of spherical grains with diameters of 175 and 225  $\mu\text{m}$  is assumed

**Table 2:** Estimation of the number of grains for 100-150  $\mu\text{m}$ , 150-200  $\mu\text{m}$  and 200-250  $\mu\text{m}$  diameter grains.

Grain size	Aliquot diameter (mm)	Estimated average number of grains	Assumed packing ratio (%)
100-150 $\mu\text{m}$	6	1406	63
	2	156	
150-200 $\mu\text{m}$	2	75	65
200-250 $\mu\text{m}$	2	46	

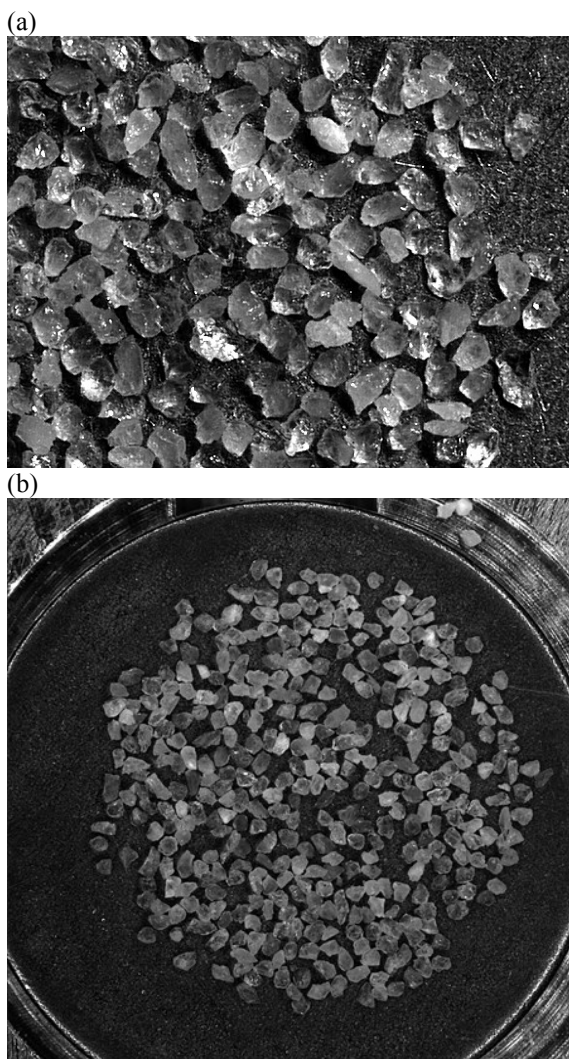


**Figure 1:** (a) 200-250  $\mu\text{m}$  grains of sample WAU-MH3 on an aliquot, (b) A view of the whole disc.

Table 1 summarises the results of counting over 50 thousand grains attached to 6 mm aliquots. The table presents the average number of grains from diameter ranges of 150-200  $\mu\text{m}$  and 200-250  $\mu\text{m}$  calculated assuming densest packing, the average counted numbers of grains, their standard deviation and the ratio of those two values (called here the ‘packing ratio’).

We found that a 6 mm aliquot of 150-200  $\mu\text{m}$  grains contains on average  $677 \pm 48$  grains and a 6 mm aliquot of 200-250  $\mu\text{m}$  contains  $440 \pm 46$  grains. As shown in the last column of Table 1 the actual number of grains on an aliquot is lower than that predicted by dense packing by at least 35%.

### Implications

Based on the results obtained from counting grains, we estimated the numbers of grains for the grain size 100-150  $\mu\text{m}$  on 6 and 2 mm aliquots, and for 150-200  $\mu\text{m}$  and 200-250  $\mu\text{m}$  diameter grains on 2 mm aliquots. These estimates are listed in Table 2. In the case of the smaller grains, we assumed the same packing ratio as in the case of 150-200  $\mu\text{m}$ , whereas for the two other ranges we used the packing ratio given in Table 1.

The experimentally determined packing ratios (Table 1) and the proportion of bright and dim grains (further jointly termed active grains) in the quartz extracts (for details and definition of “bright” and “dim” see Appendices A and B) makes it possible to estimate the probability of a given number of active grains being present on an aliquot.

The number of active grains present on an aliquot follows a binomial distribution. The probability of getting exactly  $k$  active grains on a disc ( $k$  successes) containing  $n$  grains ( $n$  trials) with a given proportion  $p$  of such grains in the total (probability  $p$ ) equals:

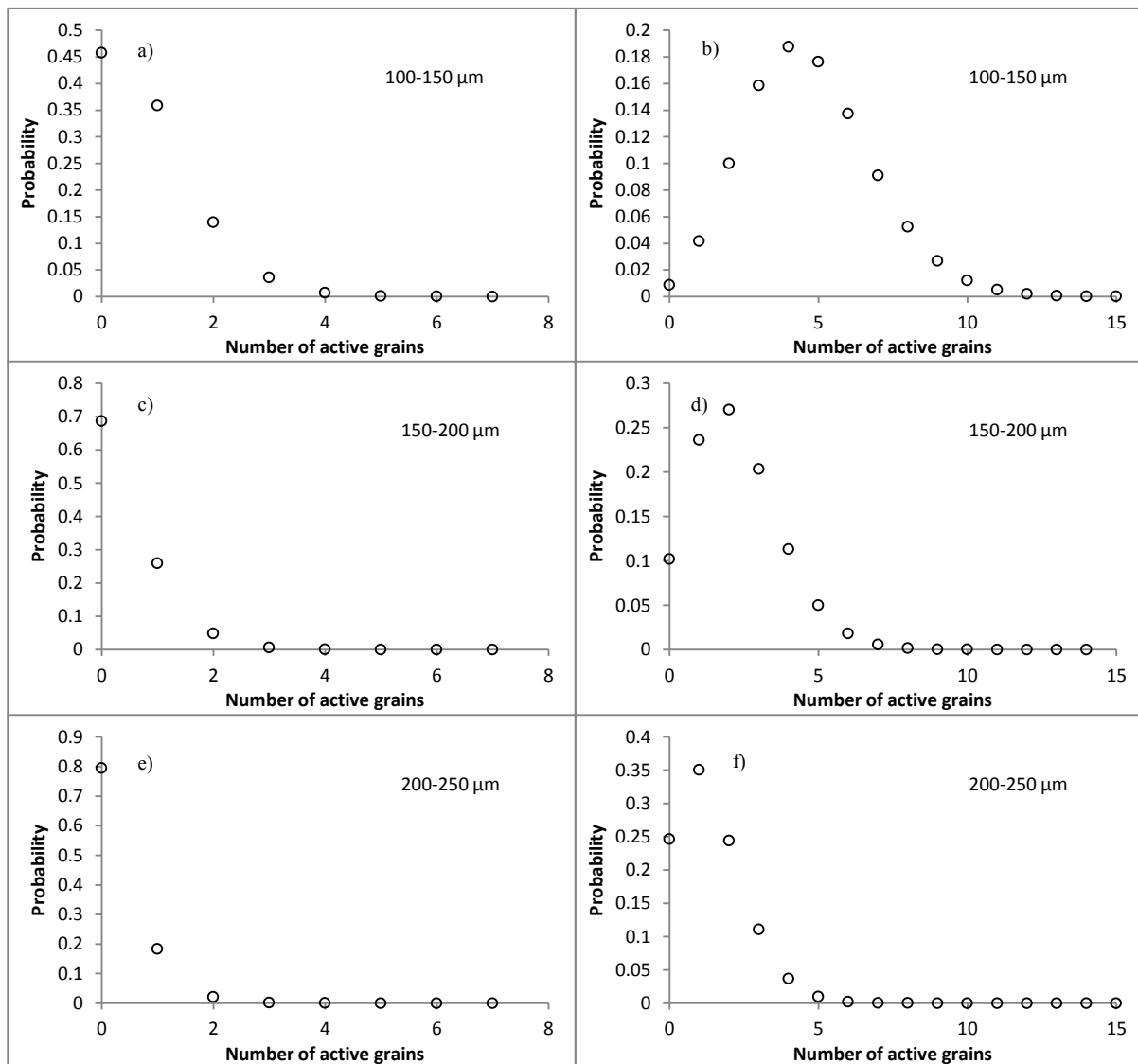


**Figure 2:** The probability of a given number of active grains on 2 mm aliquots of quartz; a), c) and e) probabilities for bright grains; b), d) and f) for dim grains.

$$P_k = \binom{n}{k} p^k (1-p)^{n-k} \tag{1}$$

Single grain measurements (see Appendix A for details) revealed that samples investigated in this study hardly contain any grains emitting light. For the calculations we assumed that only 0.5% of the grains are bright, and ~3% of the grains are dim, as defined in Appendix A. Figures 2 and 3 present the probabilities of encountering a given number of bright and dim grains on 2 mm and 6 mm aliquots, respectively. For example, 80% (probability of 0.8) of 2 mm aliquots containing 200-250 μm grains (Figure 2e) will not contain any bright grains and 25% of such aliquots will not contain any grains

emitting light at all (Figure 2f). Consequently, well over 25% of such aliquots will not emit any measurable signal, however we do not have any measurements with 250 μm 2 mm aliquots.

In the case of 6 mm aliquots, 11% will not contain any bright grains, 24% one bright grain, 27% two bright grains, 38% more than two bright grains (Figure 3e). In addition, such aliquots will contain between 5 and 25 dim grains (Figure 3f).

Taking into account the considerations presented in Appendix B it is possible to state that the signal of one 6 mm aliquot (of Alpine quartz) consists of the signal originating from a few tens of dim grains and some bright grains, however, there will be a few aliquots which will be dominated by the signal of single bright grains. Different conclusions may be

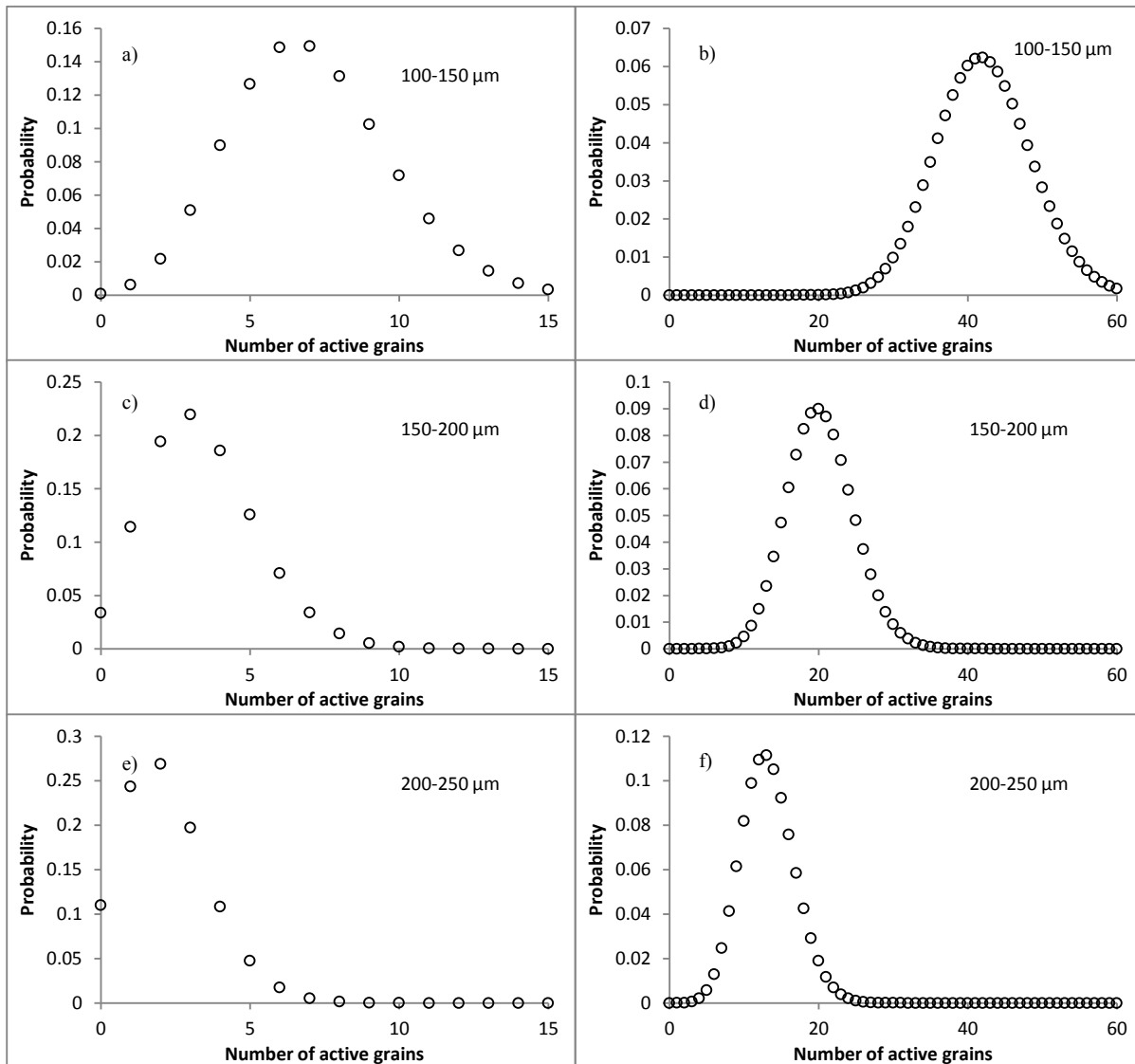


**Figure 3:** The probability of a given number of active grains on 6 mm aliquots of quartz; a), c) and e) probabilities for bright grains; b), d) and f) for dim grains

reached for another sample characterised by a different, experimentally determined, proportion of bright and dim quartz grains.

### Conclusions

In this investigation we found that a significant discrepancy existed between the theoretically calculated number of grains and the actual number of grains. We suspect that there are several factors that may affect the magnitude of such discrepancy. These factors include the technique of aliquot preparation, the person who prepares the aliquots and the size and the shape of the grains, and hence the type of sediment, length of transport and duration of grain working.

We suggest that the knowledge of the packing ratio and the proportion of active grains in a given sample are very important in the choice of the used aliquot size to optimise the proportion of active grains on a single aliquot and the counting statistics.

For a sample the proportion of active grains and the packing ratio might be important for explaining the discrepancy between single grain and single aliquot results that is sometimes observed, especially when  $D_e$  modelling is used. It would be interesting for other laboratories to perform similar checks to explore the degree of variability of the packing ratio between laboratories and between quartz of varying provenance.

## References

- Adamiec, G., Heer, A.J., Bluszcz A., in press, Statistics of count numbers from a photomultiplier tube and its implications for error estimation. *Radiation Measurements*, doi:10.1016/j.radmeas.2011.12.009
- Arnold, L.J., Roberts, R.G., 2009. Stochastic modelling of multigrain equivalent dose ( $D_e$ ) distributions: Implications for OSL dating of sediment mixtures. *Quaternary Geochronology* **4**, 204-230.
- Bailey, R.M., Yukihara, E.G., McKeever, S.W.S., 2011. Separation of quartz optically stimulated luminescence components using green (525 nm) stimulation. *Radiation Measurements* **46**, 643-648.
- Duller, G.A.T., 2008. Single-grain optical dating of Quaternary sediments: why aliquot size matters in luminescence dating. *Boreas* **37**, 589-612.
- Duller, G.A.T., Bøtter-Jensen, L., Murray, A.S., 2000. Optical dating of single sand-sized grains of quartz: sources of variability. *Radiation Measurements* **32**, 453-457.
- Rhodes, E.J., 2007. Quartz single grain OSL sensitivity distributions: implications for multiple grain single aliquot dating. *Geochronometria* **26**, 19-29.

## Appendix A

### Number of luminescent grains in quartz extract

In order to determine the number of luminescent quartz grains in the used extracts, the natural ( $L_N$ ) and the regenerated ( $L_1$ ) CW-OSL signals were measured for up to 500 single grains per sample.

The measurements were performed on automated TL/OSL-DA-20 Risø readers including a  $^{90}\text{Sr}/^{90}\text{Y}$  beta source and an EMI 9235 PM tube. Optical stimulation was carried out using a 10mW Nd: YVO<sub>4</sub> solid state diode-pumped laser emitting at 532 nm (green light). The sample was preheated for 10 s at 220°C and read out at 125°C for 1s and recorded in 0.02 s time intervals. The OSL detection was performed through a Hoya U340 filter. Before measurement, each aliquot was tested for feldspar contamination by applying an IR-shine and eliminated if any response was observed.

Figure A1.a shows the net OSL signal curves, visualising the proportion of grains emitting more than 1ct/0.02s/Gy of OSL averaged over the first 0.06s of the decay, as described by Duller (2008). The signal level of 1ct/0.02s/Gy is thought to be acceptable when calculating single grain growth curves (Prof. G. Duller, personal communication). In the case of the investigated samples only 0.5-1% of grains gave a signal higher than this threshold (Figure

A1.a). Figure A1.b, on the other hand, shows cumulative light sum curves as described by Duller et al. (2000). They indicate that apart from bright grains (ca. 60% of the luminescence), a significant part of the signal on a single aliquot originates from dim grains and some not further explored “noise” (ca. 40%) in the investigated samples. This observation differs from the frequently made assumption that mainly bright grains contribute to the measured signal. The data provided here indicate that often the signal gained from an aliquot is the sum of the signal of a few tens of grains, at least in the investigated Alpine samples. The situation will change in samples where some extremely bright grains occur. In such cases the total single aliquot signal may be dominated by the signal of such bright grains.

For the purpose of this study the threshold value dividing grains into bright and dim ones was chosen to be 80 cts in the first 0.02s channel of the OSL decay in response to a beta dose of 55 Gy – this value was selected on the basis of the considerations described in Appendix B. The brightest grains emitted a maximum of about 400 cts in the first 0.02 s channel of the OSL decay. Figures A1.c and A1.d show examples of OSL decay curves obtained from a dim and a bright grain, respectively.

## Appendix B

### Estimation of the magnitude of SG signal that can be distinguished from the background of a single multigrain aliquot

In order to estimate the magnitude of a single grain (SG) signal, measured under green light laser stimulation, necessary for the signal to be distinguishable from the background level in single aliquot (SA) measurement, using blue stimulation, we applied the following considerations.

For the ease of computation we assume that the SA signal (initial channels of the OSL decay curve) consists of the fast component of a SG and a background, which may consist of slow components and the PM tube background. The medium component is neglected. In addition, as this is a rough estimation, we ignore  $k_{corr}$ , described in Adamiec et al. (in press) and assume a Poisson distribution of the count numbers.

If the measured CW OSL of a single aliquot (SA) is  $S$  (understood as counts summed over time  $t_s$ ) and the background to be subtracted is  $B$  (understood as background estimated on the basis of the last integral) then the OSL signal sum from the grain(s) is  $I=S-B$ . The uncertainty ( $u$ ) of this signal is

$$u(I) = \sqrt{u^2(S) + u^2(B)} \quad (1.1)$$

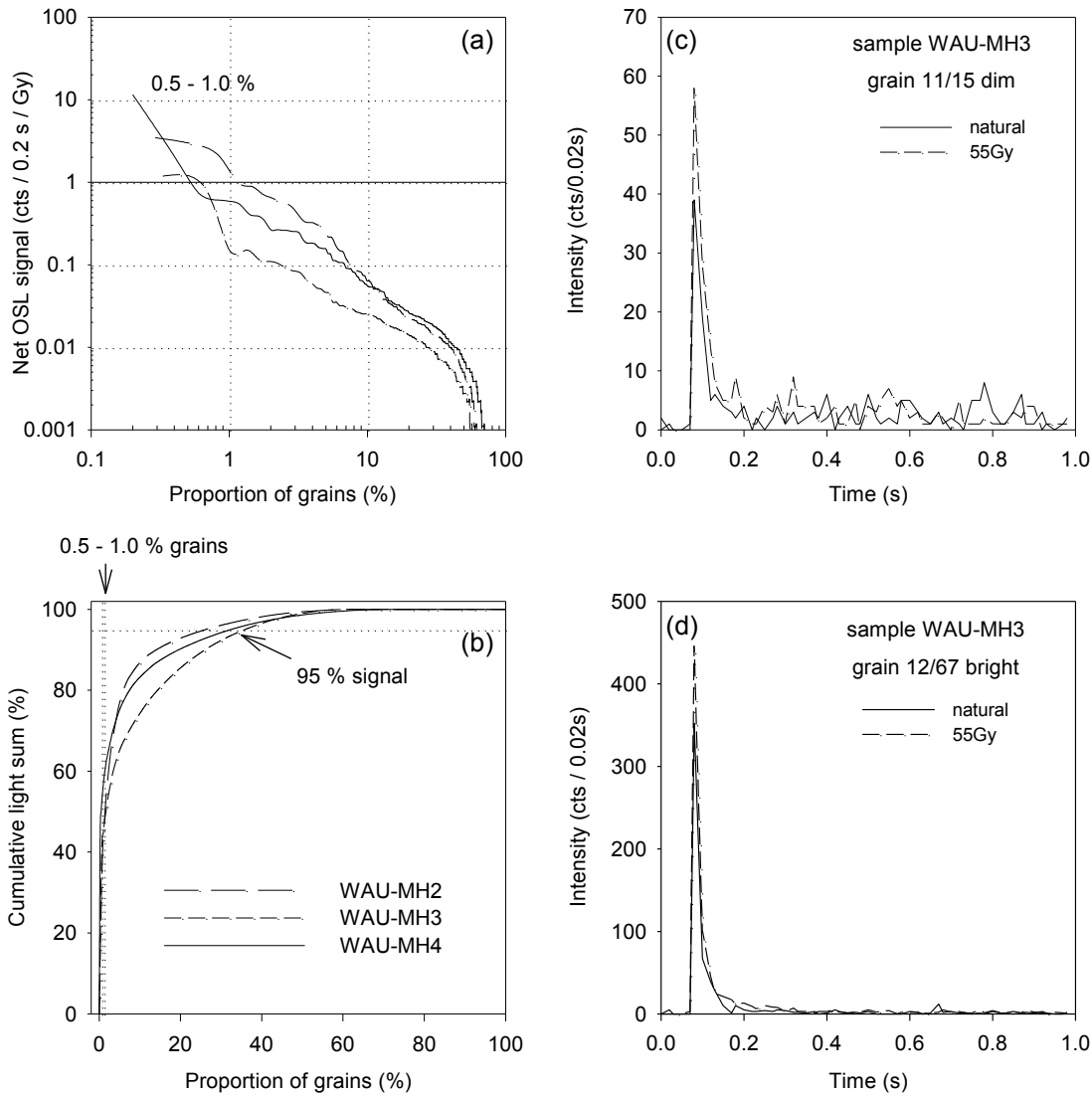


**Figure A1:** Determination of the number and the quality of luminescent grains in the Wauwilermoos samples: a) net OSL curves (as defined in Duller 2008); b) cumulative light sum curves (as defined in Duller et al. (2000)) for samples WAU-MH2, WAU-MH3 and WAU-MH4; c and d) examples of OSL decay curves of the natural (solid line) and regenerated (dashed line) single grain OSL for a dim (c) and bright (d) quartz grains from sample WAU-MH3.

If we assume that the count numbers are distributed according to the Poisson distribution this becomes

$$u(I) = \sqrt{S + B \cdot c} \quad (1.2)$$

where  $c = \frac{t_S}{t_B}$  and  $t_S$  and  $t_B$  are the time of signal

integration and background integration, respectively.

In order for the signal  $I$  to be distinguishable from the background the OSL signal should exceed its standard deviation and thus the following condition must be fulfilled

$$I > k \cdot u(I),$$

where  $k$  would be usually selected to be 2 or 3.

The OSL measured is  $S$  and it is numerically equal to  $B+I$ , where  $I$  is the signal originating from a grain assuming that the SA signal consists of background and OSL emitted by one grain. If we combine the above equations we obtain

$$I > k \sqrt{B(1+c) + I}$$

This gives us the quadratic condition

$$I^2 - k^2 I - k^2(1+c)B > 0$$

**Table B.1:** A summary of estimated  $I$  and signal necessary to distinguish a single grain's signal superimposed on the background of a multigrain aliquot for different values of parameters

Background rate ( $s^{-1}$ )	1500	1500	80	80	1500	1500	80	80
$k$	3	3	3	3	2	2	2	2
$t_s$	0.2	1	0.2	1	0.2	1	0.2	1
$t_B$	10	10	10	10	10	10	10	10
$c$	0.02	0.1	0.02	0.1	0.02	0.1	0.02	0.1
$B$	300	1500	16	80	300	1500	16	80
$I$	<b>57</b>	<b>126</b>	<b>17</b>	<b>33</b>	<b>37</b>	<b>83</b>	<b>10</b>	<b>21</b>
$S = I+B$	<b>357</b>	<b>1626</b>	<b>33</b>	<b>113</b>	<b>337</b>	<b>1583</b>	<b>26</b>	<b>101</b>

Solving this and rejecting the negative value finally gives the condition for the signal of a single grain to be distinguishable from the background of a SA

$$I > \frac{k^2 + \sqrt{k^4 + 4k^2(1+c)B}}{2} \quad (1.3)$$

Table B.1 summarises a few examples of calculated values of count numbers originating from grains in order to make them distinguishable from the background. For example, if we take into account the first second of the OSL decay curve, the background is estimated using the last 10 s of the decay curve we have  $c=1/10=0.1$ ,  $B$  for 1 s equals 1500 (such a value was measured for sample WAU-MH3 due to a large slow component contribution). Choosing  $k=3$  gives  $I=126$  counts and  $S=1626$  counts, while for  $k=2$   $I=83$  and  $S=1583$ .

In order to compare this with the signal of a single grain under green laser stimulation we need to take into account the power of stimulation and the difference in the cross section for interaction of trapped electrons due to the different wavelengths. The typical power of blue light stimulating diodes (470 nm, photon energy 2.53 eV) is of the order of 50 mW/cm<sup>2</sup>, while the power of the stimulating laser in single grain measurements (green light, 532 nm, photon energy 2.23 eV) is about 50 W/cm<sup>2</sup>, giving a photon flux ca. 1000 times higher in the case of the laser stimulation.

The cross section for interaction with 470 nm photons is equal to  $\sigma_{\text{fast}}=2.25 \times 10^{-17}$  cm<sup>2</sup> (calculated using the formulae given in Bailey et al., 2011; see Fig. 1 therein; more precise values of parameters needed to calculate the cross sections were supplied by Dr. R. Bailey, pers. comm.) and hence the decay time constant for blue light for a power of 50 mW/cm<sup>2</sup> is equal to 0.38 s which means that for a

single aliquot measurement practically the whole fast component is emitted in the first second of decay. On the other hand, in the case of SG measurements using green light,  $\sigma_{\text{fast}}=3.48 \times 10^{-18}$  cm<sup>2</sup> and the decay time constant is 2.2 ms. Therefore the whole of the fast component will be emitted during the first 0.007 s (the decay in case of SG green light measurements is ca. 170 times faster than in the case of SA blue light measurements). This means that the whole of the fast component is measured practically in the first channel only, as typically in single grain measurements channels of length 0.02 s are used. On this occasion it is worth noting that similar considerations made for the medium component return the decay time constant of 2.03 s for SA measurements and 0.025 s for SG measurements which means that the medium component will be practically emitted within the first 0.08 s in SG measurements.

All this information combined, under the assumption (for ease of computation) that the background in SG measurements gives negligible contribution, as it is often observed, leads to the conclusion that if one single grain of the dim Alpine quartz were to be seen above the high background of a single aliquot on a 2  $\sigma$  level it would have to show more than about 80 counts (6<sup>th</sup> column in Table B.1) in the first channel of the SG measurement. In the case of the 6 mm aliquots with a background equal to the machine background (let's assume 80 counts per second), this would amount to 21 counts for the single grain to be distinguishable (in Alpine samples there is always a high slow component contribution so this is a hypothetical situation).

These back-of-the-envelope calculations are a rough estimate and in order to check them one would have to select a bright grain and after irradiation place it on an aliquot to see whether this holds true.

We decided to classify the grains using the limit of 80 counts in the first channel of the SG OSL decay curve qualifying grains brighter than this limit as 'bright' grains while grains emitting a lower signal, though with a detectable OSL decay, as 'dim' grains.

**Reviewer**

K.J. Thomsen

# Towards a SAR-ITL protocol for the equivalent dose estimate of burnt quartzites

C. Tribolo\* and N. Mercier

Institut de Recherche sur les Archéomatériaux, UMR 5060 CNRS - Université de Bordeaux, Centre de Recherche en Physique Appliquée à l'Archéologie (CRP2A), Maison de l'archéologie, 33607 Pessac cedex, France

\*corresponding author: ctribolo@u-bordeaux3.fr (C. Tribolo)

(Received 9 March 2012; in final form 31 May 2012)

## Abstract

Up to now, the preferred protocol for determining the Equivalent Dose ( $D_e$ ) of burnt lithics has been a multiple aliquot additive and regenerative dose (MAAD) approach based on the measurement of the thermoluminescence (TL) signal. The purpose of this study was to test a single aliquot regenerative dose (SAR) protocol measuring the isothermal thermoluminescence (ITL) signal. It is shown that this protocol is efficient for quartzites where the TL glow curve is dominated by the 280 and 375°C peaks. However, it fails with quartzites for which the relative contributions of TL peaks change with regenerative doses.

## Introduction

Up to now, the determination of the equivalent dose ( $D_e$ ) for burnt rocks (either flints or quartzites) has been done using the thermoluminescence signal (TL) at 370–380°C (for a heating rate of  $\sim 5^\circ\text{C}\cdot\text{s}^{-1}$ ) and by applying mainly multiple-aliquot additive and regenerative dose (MAAD) protocols. Meanwhile, it is well known that multiple aliquot approaches present several drawbacks (in comparison with single aliquot approaches, e.g. Murray and Wintle, 2000), such as: 1) the large amount of material needed for obtaining one  $D_e$  estimate, 2) the lack of systematic controls for accuracy such as dose recovery tests (Richter and Temming, 2006), 3) the difficulties in correctly extrapolating the TL growth curve to a zero signal, more particularly when the  $D_e$  is close to saturation, and 4) the low reproducibility of the measured TL signals sometimes seen for a given dose.

Attempts at using TL single aliquot protocols for the  $D_e$  determination of flints have been performed through detecting their UV-blue emission (Valladas, personal comm.), but were not successful due to the impossibility of satisfactorily correcting for the sensitivity changes occurring in most samples during

the first heating in the laboratory. Richter and Temming (2006) and Richter and Krebschek (2006) were quite satisfied however with a TL short SAR procedure (single aliquot regenerative dose protocol, without any test dose measurements) for flints in detecting their orange emission as they observed that, in most cases, the sensitivity changes were low enough to be neglected. These authors also tested a protocol using isothermal measurement of the TL (ITL) in various wavelength ranges (UV-blue, orange–red and full spectrum) either with standard SAR or short SAR procedures. In a minority of cases only the SAR-ITL dose recovery ratios were close to unity at one sigma. Finally, these authors concluded that the standard MAAD-TL protocol in which the UV-blue emission is selected (Valladas, 1992) remains the best choice for flint dating.

Beyond these attempts focusing on burnt flints, studies using SAR-ITL protocols have been performed on sedimentary quartz grains with signal detection in the UV range and on volcanic materials with ITL detected at red wavelengths (Wintle 2010 and references therein). The main purpose of these studies was to extend the quartz dating range, as it was noticed that the ITL signal saturates at higher doses than the optically stimulated luminescence (OSL) signal (Murray and Wintle, 2000). Experiments on the origin, bleachability, thermal stability and dose response of the ITL signal have been performed at different temperatures (e.g. Jain et al., 2005, 2007 a and b), and various SAR-ITL protocols have been tested by different authors (Table 1). Choi et al. (2006) and Jain et al. (2005) (also see Gibling et al., 2005) obtained satisfying results with ITL measurements at 310 or 320°C, but Huot et al. (2006) and Buylaert et al. (2006) both noted that their SAR-ITL protocol (also at 310°C) is inefficient for their samples: a sensitivity change occurring during or just after the measurement of the natural signal is not properly corrected for by the following test dose.

**Table1:** Summary of the different SAR-ITL protocols that have been proposed. In all cases but Barham et al. (2011), the same heat treatment is done for the natural and regenerative doses and for the test doses.

Reference	Murray and Wintle (2000)	Jain et al. 2005; Gibling et al. 2005	Choi et al. 2006	Huot et al. 2006	Buylaert et al. 2006	Richter and Temming 2006	Vanderberghe et al. 2009	Pagonis et al. 2011	Barham et al. 2011
Material	Fluvial quartz	Fluvial or aeolian quartz from Indo-Gangetic plain	Various sedimentary quartz	Various sedimentary quartz	Chinese loess	Flint	Various sedimentary quartz	Simulation	Quartz from river bench in Zambia
Wavelength	UV	UV	UV	UV	UV	Various	UV		
Heating Rate		2°C/s	5°C/s	5°C/s	5°C/s	5°C/s	2°C/s	5°C/s	
Preheat	340°C cut, OSL at 330°C for 5s	No	310°C for 10 s	No	No	350°C cut	300°C for 10s	300°C for 10s	280°C for 10s
Protocol	ITL	320°C for 500s	310°C for 500s	310°C for 100s or 300s	310°C for 300s	340°C for 500s	270°C for 600s	310°C for 600s	310°C for 250s except for the natural: 310°C for 3s + 110 min bleaching in solar simulator
Cleaning	no	no	no	no	no	no	OSL 280°C for 40s	OSL 280°C for 40s	no
Notes		Works fine for most; for some samples sensitivity change during 1 <sup>st</sup> measurement is suspected		Sensitivity change during 1 <sup>st</sup> measurement	Sensitivity change during 1 <sup>st</sup> measurement. SARA preferred	Accurate at 2 sigma only		Sensitivity change during 1 <sup>st</sup> measurement	

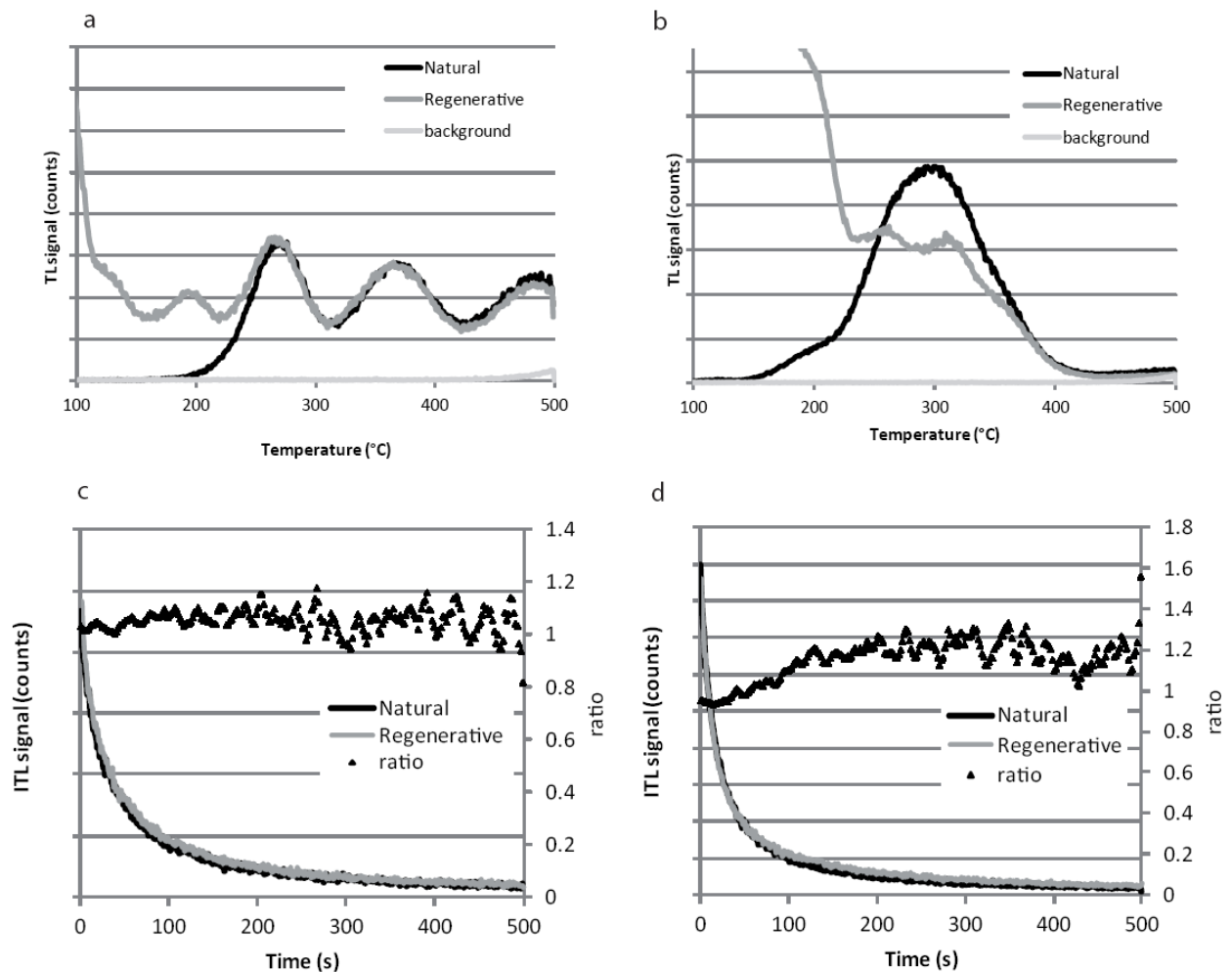


**Figure 1:** Natural, regenerative and background TL glow curves obtained when the temperature is increased at 5°C/s. a) DRS178, b) DRS196. Natural and regenerative ITL decay curves at 300°C after a 10s preheat at 300°C. The ratio between the two curves is also plotted; c) DRS178, d) DRS196.

This effect has also been observed by Pagonis et al. (2011) for simulated SAR-ITL experiments. To get round this problem, three kinds of solutions have been proposed: 1) allowing for this initial sensitivity change with a Single Aliquot Regenerative and Additive dose (SARA) protocol (Buylaert et al., 2006), 2) minimizing the sensitivity changes by working with lower temperatures (Vandenberghé et al., 2009), or 3) by replacing the long heat of the natural by a short heat (3 s only instead of 250 s for the test and regenerative doses) followed by an optical bleaching in a solar simulator (Barham et al., 2011). It is not clear whether the successes or failures obtained within the cited works are due to differences in the protocols or to samples that may or may not stand the SAR-ITL protocols. Meanwhile, as the main problem that was identified for these bleached

sedimentary quartz seemed to be linked with the first heating of the sample, it is possible that it would be less stringent for quartz that were already submitted to a high temperature heat (at least 350°C) in the past. The purpose of this paper is to present SAR-ITL tests performed on such burnt quartzites.

### Samples and Measurements

The quartzite samples come from Diepkloof Rock Shelter (South Africa), a thick Middle Stone Age deposit (Parkington et al., in prep; Porraz et al., in prep; Texier et al., 2010; Tribolo et al., 2009, in prep). The samples can be described as a cluster of quartz grains, the granulometric distribution of these grains varies from sample to sample. The core of each quartzite was sawed and crushed so that a quartz

powder with an artificial grain size of 100-160 $\mu$ m was obtained.

Measurements were performed with a TL/OSL DA15 Risø reader, equipped with an EMI Q9235 photomultiplier tube, preceded by a combination of Schott BG39 and Corning 7-59 filters for detection in the UV-blue wavelength range (about 330-450 nm). A  $^{90}\text{Sr}/^{90}\text{Y}$  beta source was used for irradiations and the heating rate was  $5^\circ\text{C}\cdot\text{s}^{-1}$  for all experiments.

Based on the observation of the natural and regenerative TL glow curves, two groups of samples can be distinguished: in the first group, the natural TL signal presents two peaks at 280 and 375 $^\circ\text{C}$  (the 325 $^\circ\text{C}$  peak being likely dominated by this last one), and the shape of the regenerative glow curve is similar to the natural one above 280 $^\circ\text{C}$  (e.g. DRS178 on Figure 1a). For the second group, the 325 $^\circ\text{C}$  peak contributes significantly to a broad signal dominating the first glow curve but its relative contribution (in comparison with the 280 and 375 $^\circ\text{C}$  peaks) is different in the regenerative curve. This allows us to distinguish these three peaks but as a consequence, the natural and regenerative glow curves are not homothetic (e.g. DRS196 on Figure 1b). It is therefore unreasonable to combine the growth curves built from the additive and regenerative TL glow curves in order to determine the  $D_e$  of these samples. Therefore, when MAAD protocols are applied, the samples from this group are usually discarded (which represents about 45% of burnt stones from Diepkloof). Figure 1c and d display natural and regenerative ITL glow curves recorded at 300 $^\circ\text{C}$  for samples DRS178 (first group) and 196 (second group) respectively, following a 10s preheat at 300 $^\circ\text{C}$ . In both cases, the regenerative and natural decay curves seem very similar, though calculation of the ITL signal ratio reveals that the curves are not perfectly homothetic for DRS196, with a 10% increase during the first 100 s. Nonetheless, the question behind this is whether using an ITL protocol instead of a TL one could avoid the need to discard group 2 samples from the dating process.

The SAR-ITL protocol used in our experiments is presented in Figure 2. Each cycle is composed of the following steps: after irradiation, a 10s preheat at temperature T is applied and the ITL measurement is performed at the same temperature for 500 s. A 52 Gy test dose is given and the same preheat and ITL measurements are performed once again. A 500 $^\circ\text{C}$  TL measurement has been included at the end of each cycle to avoid signal build-up (data not shown). This cycle is repeated for regeneration doses of D, 2D, 4D, 8D, 0, D and 8D, where D is close to the expected  $D_e$ . Unless otherwise specified, the first 20 s and the last 50 s of the ITL signals were considered as signal and background, respectively.

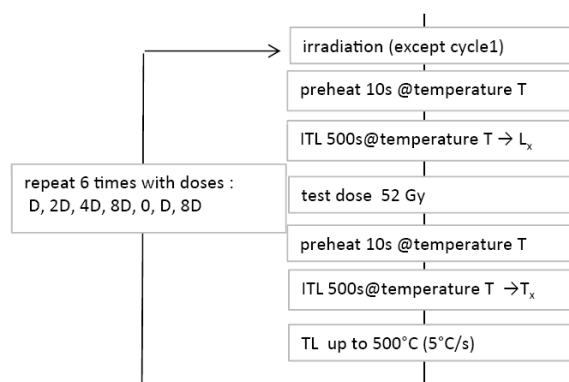


Figure 2: SAR-ITL protocol.

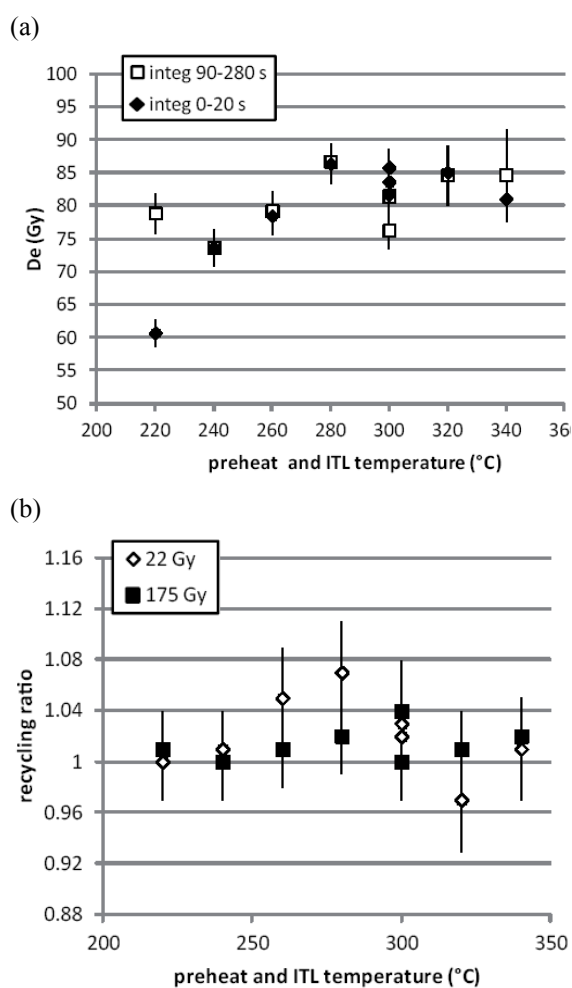


Figure 3: a) SAR-ITL  $D_e$  values as a function of preheat and ITL temperature for DRS178. Signal is integrated either over the first 20s (black diamonds) or over the 90-280s interval (the last 50 s are used for background in both cases). b) recycling ratios for the SAR-ITL experiment as a function of the preheat and ITL temperature (integration: first 20s).

### Study of samples from group 1

#### SAR -ITL

Figure 3a shows the  $D_e$  as a function of the temperature  $T$ , which was varied between 220 and 340°C by steps of 20°C, for sample DRS178<sup>1</sup>. Figure 3b displays the corresponding recycling ratios for the lowest and highest regenerative doses. These ratios are all consistent with unity at one or two sigma whatever the temperature, showing that the sensitivity correction is efficient at least from the second cycle. Meanwhile, the calculated  $D_e$  values increase from 240 to 280°C (Figure 3a) and then remain constant up to 340°C (mean  $D_e$  on 280-340°C: 84±3Gy), whatever the integration interval: the  $D_e$  obtained when integrating a later part of the signal (e.g. 90-280s) is consistent at one sigma with the  $D_e$  estimates obtained for the first 20s, except at 220°C. Experiments that were carried out in order to correlate the ITL and TL signals suggest that at 220°C, the ITL signal can be entirely associated with the 280°C TL peak (data not shown), while above this temperature, the ITL signal is dominated by the 325° and 375°C TL peaks. As the 280°C TL peak is known to be unstable at long timescales (>10ka; Spooner and Questiaux, 2000), it is therefore not surprising that the apparent  $D_e$  decreases when its contribution to the ITL signal increases.

While observing that the  $D_e$  is not dependent on the temperature at least between 280 and 340°C is satisfying, it does not ensure that the obtained  $D_e$  is correct. A dose recovery test was thus performed in order to check for the efficiency of the protocol: the signal was zeroed by heat (450°C for 1h30min)<sup>2</sup>, a known dose close to the expected  $D_e$  was given and the protocol was applied for a temperature of 320°C. One aliquot of DRS178 was tested and yielded a good recovery (estimated to expected dose) ratio of 1.01±0.03.

#### SARA -ITL

Huot et al. (2006) and Buylaert et al. (2006) noticed that the sensitivity change occurring during the first heat (ITL measurement) was not properly corrected for by the use of a test dose, but this correction was working fine for the following cycles. It was therefore feared that the dose recovery test performed

<sup>1</sup> Note that we used here a cut edge of the stone, which was submitted to beta and alpha radiations from the surrounding sediment. The  $D_e$  of this part is therefore different from the  $D_e$  obtained for the core, presented in Tribolo et al., (in prep).

<sup>2</sup> 450°C is the temperature indicated by the thermocouple of the oven. The actual temperature within the sample, measured with a thermocouple in contact with the quartz powder, is somewhat different: rapid increase from 20 to 200°C in <5min, 340°C reached by 30min, 390°C reached by 1h00 and 400°C by 1h30.

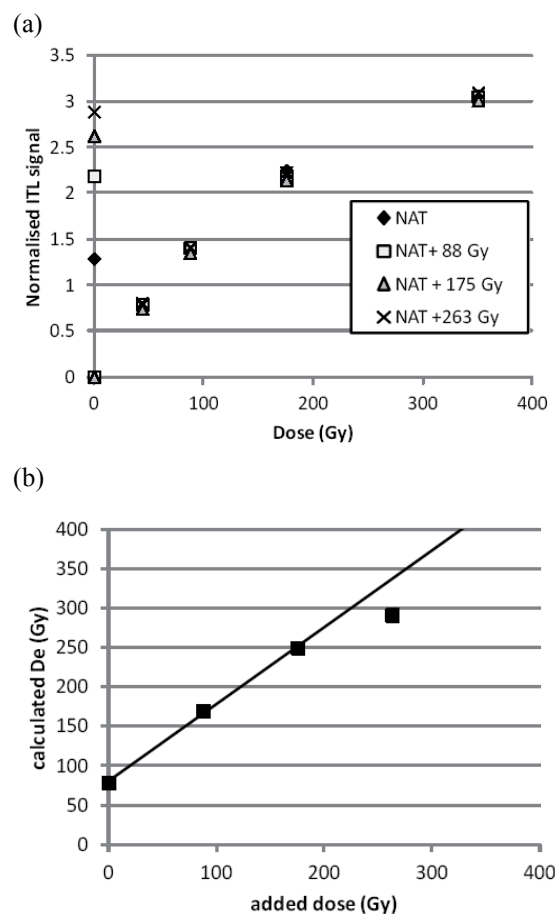


**Figure 4:** a) SAR-ITL growth curves built for testing a SARA protocol with sample DRS178 (ITL and preheat temperature: 300°C). The  $L_x/T_x$  signals for the natural and natural+added doses are projected on the interpolated growth curve. b) The estimated equivalent doses are then plotted as a function of the added doses.

in the previous section was somewhat biased since the resetting was done by heating the sample. As suggested by Buylaert et al. (2006), a SARA protocol would help answer this question since it allows the very first sensitivity change to be taken into account (assuming that all aliquots are affected by the same sensitivity change). It was then attempted on DRS178. Four aliquots were used, on which the SAR-ITL protocol at 300°C was applied, except that doses of 88, 175 and 263 Gy were added to the natural dose for three out of the four aliquots (Figure 4a). For each aliquot, the estimated dose was then plotted as a function of the added dose (Figure 4b). For the SARA protocol to be successful, the growth curve has to remain linear. In this condition, the intercept on the Y axis of the  $D_e$  versus added dose straight line corresponds, when it is divided by the slope of this line, to the corrected  $D_e$  (Mejdahl and Bøtter-Jensen, 1994).

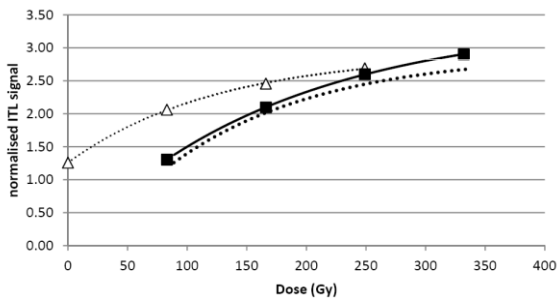


**Figure 5:** Additive (white triangles) and regenerative (black squares) growth curves obtained with multiple aliquots for sample DRS178. The bold dotted line represents the additive growth curve after slide.

On Figure 4a, it can be seen that the growth curve is linear in the dose interval lower than 200 Gy. Consequently, only the three added doses of 0, 88 and 175 Gy were considered for the  $D_e$  calculation (Figure 4b). The computation of the slope indicated that its value is close to unity ( $0.97 \pm 0.02$ ) and the corrected SARA  $D_e$  was found to be  $86 \pm 2$  Gy, consistent with the  $D_e$  estimated with the SAR-ITL protocol ( $84 \pm 3$  Gy), suggesting that for this sample there was no sensitivity change during the natural measurement cycle.

#### MAAD-ITL

As an alternative to the SARA protocol, a multi aliquot (MAAD) approach was also attempted. Four aliquots of DRS178 were used for building an additive dose growth curve (added doses: 0, 83, 146 and 249 Gy), while a regenerative growth curve was built with four other aliquots (signal reset with a  $500^\circ\text{C}$  cut heat reached at  $5^\circ\text{C}\cdot\text{s}^{-1}$ , regenerative doses: 83, 166, 249 and 332 Gy) (Figure 5). Since only one signal per dose was available, each one was attributed a  $\pm 5\%$  uncertainty (this value being likely higher than the reproducibility of our machine for this type of measurements). For calculating the  $D_e$ , both slide and extrapolation methods were used with either a quadratic or a saturating exponential fit. The  $D_e$  estimates obtained with the extrapolation methods have large uncertainties ( $77 \pm 22$  Gy for the quadratic fit,  $73 \pm 19$  Gy for the exponential fit) and are therefore not informative. When slide methods are used, the  $D_e$  estimates are  $87 \pm 8$  Gy whatever the fitting model and are consistent with the  $D_e$  estimated with SAR-ITL or SARA-ITL protocols, indicating that all the ITL procedures (based on single or multiple aliquots) lead to equivalent results.

#### Application to other samples from group 1

SAR, SARA and MAAD-ITL protocols give consistent results for DRS178, suggesting the sensitivity corrections in SAR are effective and thus,

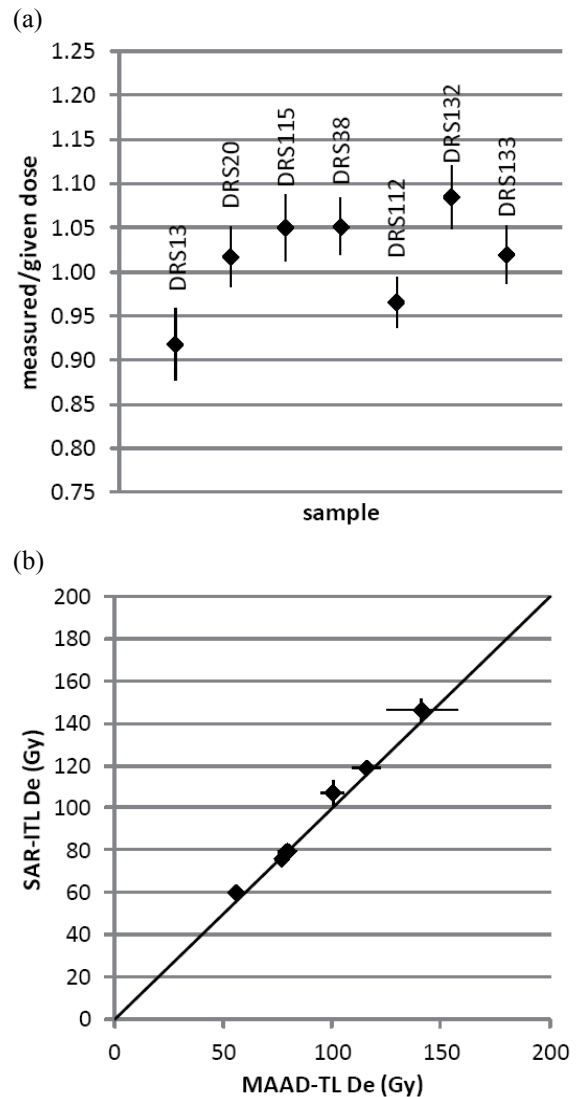


**Figure 6:** Application of the SAR-ITL protocol to seven samples from group 1. a) dose recovery ratios for one aliquot per sample (mean:  $1.02 \pm 0.05$ ). b) Comparison of the SAR-ITL and MAAD-TL  $D_e$  values for these samples (slope:  $1.05 \pm 0.04$ ).

that the  $D_e$  is accurate. In order to extend this observation, the SAR-ITL protocol was also applied to 7 samples from group 1 for which the  $D_e$ , within a 50-150 Gy interval, had been previously measured with a MAAD-TL protocol (Tribolo et al., in prep). Figure 6a displays the dose recovery ratios obtained for one aliquot of each sample with this protocol (preheat and ITL temperature at  $320^\circ\text{C}$ ). They are all within 10% of unity. The SAR-ITL was then applied to these samples for temperatures between 280 and  $340^\circ\text{C}$ . As for DRS178, the  $D_e$  is both independent of the temperature for all samples (except DRS38, 112, 132 for which this interval is restricted to  $300\text{--}340^\circ\text{C}$  only) and of the integration zone. In all cases, the

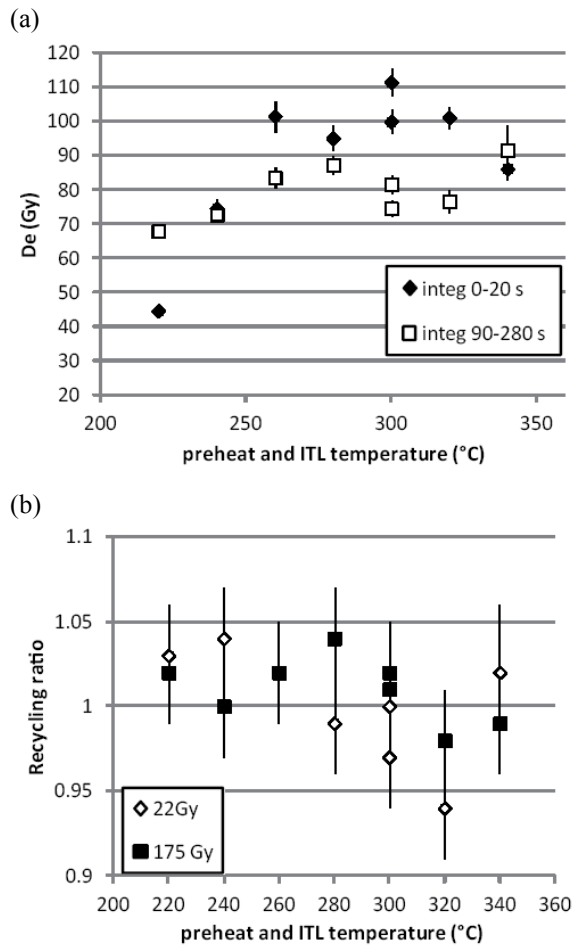


**Figure 7:** a) SAR-ITL  $D_e$  as a function of the preheat and ITL temperature for sample DRS196. Signal is integrated either over the first 20s (black diamonds) or over the 90-280s interval (the last 50 s are used for background in both cases). b) recycling ratios for the SAR-ITL experiment as a function of the preheat and ITL temperature (integration: first 20s).

recycling ratios are within 10% of unity (data not shown). On Figure 6b, the SAR-ITL  $D_e$  estimates are plotted as a function of the MAAD-TL  $D_e$  values. The agreement is very satisfying, all points being consistent at one sigma with the 1:1 line.

**Study of samples from group 2**  
 SAR-ITL

The SAR-ITL protocol that was successfully tested on DRS178 and other samples from group 1 was applied to DRS196. The apparent  $D_e$  values are plotted on Figure 7a as a function of the preheat and ITL temperature. They increase from 220 to 260°C, then are consistent at one sigma up to 320°C (mean

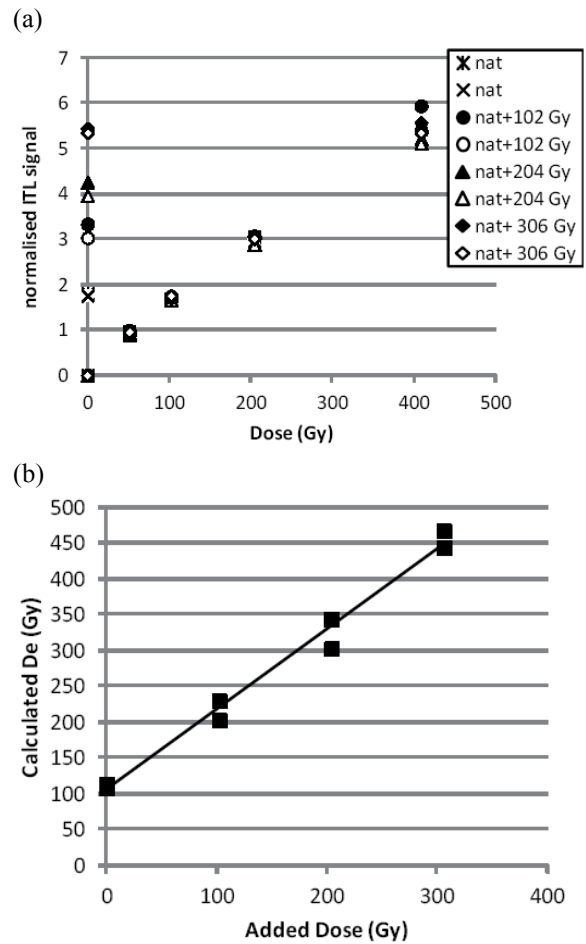


**Figure 8:** a) SAR-ITL growth curves built for testing a SARA protocol with sample DRS196 (ITL and preheat temperature: 300°C). The  $L_x/T_x$  signals for the natural and natural+added doses are projected onto the interpolated growth curve. b) The estimated equivalent doses are then plotted as a function of the added doses.

102±4 Gy) and apparently decrease again at 340°C. The recycling ratios are consistent with unity whatever the temperature (Figure 7b). However, it can be noticed that, contrary to DRS178, the  $D_e$  values obtained with a later part of the ITL signal (e.g. 90-280s: mean 81±4 Gy) are generally lower than those obtained for the first 20s, despite the recycling ratios being consistent with unity in these cases as well. It is therefore likely that the sensitivity correction is not efficient for the entire signal, maybe because this signal is composed of several components (Figure 1b).

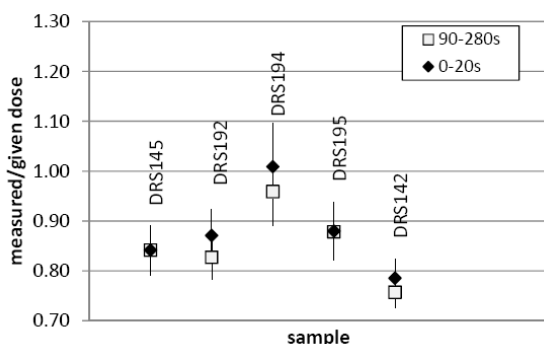


**Figure 9:** Dose recovery ratios for samples of group 2 obtained with a modified SAR-ITL protocol (after Vandenberghe et al., 2009) (mean and standard deviation for the 0-20s interval:  $0.88 \pm 0.07$ ).

#### SARA-ITL

The SARA-ITL protocol was thus applied to four aliquots of DRS196 (preheat and ITL temperatures fixed at  $300^{\circ}\text{C}$ ). The growth curve is almost linear (Figure 8a), and so is the curve describing the  $D_e$  value as a function of the added dose (Figure 8b), suggesting that the sensitivity change is the same for each aliquot. The slope of this last curve is consistent with unity at three sigma only ( $1.12 \pm 0.05$ ) confirming that the sensitivity correction of each aliquot is not efficient. When a later part of the signal is integrated, the slope is significantly lower than unity (e.g.  $0.68 \pm 0.03$  for 20-240 s), suggesting that the sensitivity change during the first measurement is even more important. The corrected  $D_e$  values for the 0-20s and 20-240s intervals are  $96 \pm 10$  and  $132 \pm 10$  Gy respectively, i.e. they are consistent with each other at 2 sigma only, indicating that for this sample the SARA protocol does not allow the recovery of the correct  $D_e$ .

#### Other protocols

The SAR-ITL protocol apparently failed because of uncorrected sensitivity changes during the first measurements. In order to minimize this effect, Vandenberghe et al. (2009) proposed applying a preheat at  $310^{\circ}\text{C}$  for 10s and performing the ITL measurement at  $270^{\circ}\text{C}$  only. A dose recovery test for this protocol was attempted on five samples of group 2 (DRS 142, 145, 192, 194, 195), except that the optical cleaning at  $280^{\circ}\text{C}$  between each cycle suggested by Vandenberghe et al. (Table 1) was replaced by a  $500^{\circ}\text{C}$  cut-heat. For the five samples, the recycling ratios were within 10% of unity (data not shown) and the  $D_e$  values were not dependent on the integration zone of the ITL signals. However for 4 out of 5 samples, the dose recovery ratio was not consistent with unity at two sigma, showing that this

modified SAR protocol is inefficient for most of our samples (Figure 9).

Finally, as single aliquot protocols did not yield satisfactory results, a MAAD-ITL protocol was attempted with sample DRS142, in which a test dose and its induced ITL signal was used for normalization. These measurements showed that the test dose signal increases with the added dose, indicating a predose effect. This effect might partly explain the failure of the SAR protocols, though it does not seem to occur in all samples (e.g. it does not with DRS196).

#### Conclusions

It has been shown that the SAR-ITL protocol is generally accurate for samples of group 1 (i.e. with dominant peaks centered at  $280^{\circ}\text{C}$  and  $375^{\circ}\text{C}$ , showing no strong change of glow curve shape after a regenerative dose is given). In future works however, the efficiency of the protocol will be systematically tested for each new sample of this group, based - as for standard SAR-OSL protocols - on dose recovery tests, dose recycling tests, preheat and ITL temperatures plateau tests, and independence of the  $D_e$  on the signal integration zone.

It can be noticed that the preheat for 10 s before the ITL measurement was maintained in this work, while several authors have suggested that this might be useless, since the ITL itself contains a heating ramp (e.g. Jain et al., 2005). The effect of removal of the preheat will be tested in future works.

Up to now, no satisfying protocol has been found for group 2 samples (i.e. samples whose glow curve shape for regenerative doses is significantly different from the natural). Pagonis et al. (2011) recommended examining the size of the test dose. Ongoing preliminary tests also suggest that the use of a lower heating rate (e.g.  $1^{\circ}\text{C}\cdot\text{s}^{-1}$  instead of  $5^{\circ}\text{C}\cdot\text{s}^{-1}$ ) could be a way to explore, but further analyses are needed before strong conclusions can be drawn.

#### References

- Barham, L., Phillips, W.M., Maher, B.A., Karloukovski, V., Duller, G.A.T., Jain, M., Wintle, A.G., 2011. The dating and interpretation of a Mode 1 site in the Luangwa Valley, Zambia. *Journal of Human Evolution* **60**, 549-570.
- Buylaert, J.-P., Murray, A.S., Huot, S., Vriend M.G.A., Vandenberghe, D.M., De Corte, F., Van den Haute, P., 2006. A comparison of quartz OSL and Isothermal TL measurements on chinese loess. *Radiation Protection Dosimetry* **119**, 474-478.
- Choi, J.H., Murray, A.S., Cheong C.-S., Hong D.G., Chang, H.W., 2006. Estimation of equivalent

- dose using quartz isothermal TL and the SAR procedure. *Quaternary Geochronology* **1**, 101-108.
- Gibling, M.R., Tandon, S.K., Sinha, R., Jain, M., 2005. Discontinuity -bounded alluvial sequences of the Southern Gangetic Plains, India: aggradation and degradation in response to monsoonal strength. *Journal of Sedimentary Research* **75**, 369-385.
- Huot S., Buylaert J.-P., Murray, A.S., 2006. Isothermal thermoluminescence signals from quartz. *Radiation Measurements* **41**, 796-802.
- Jain, M., Bøtter-Jensen, L., Murray, A.S., Denby, P.M., Tsukamoto, S., Gibling, M.R., 2005. Revisiting TL: Dose measurement beyond the OSL range using SAR. *Ancient TL* **23**, 9-24.
- Jain, M., Bøtter-Jensen, L., Murray, A.S., Essery, R., 2007a. A peak structure in isothermal luminescence signals in quartz: Origin and implications. *Journal of luminescence* **127**, 678-688.
- Jain, M., Duller, G.A.T., Wintle, A.G., 2007b. Dose response, thermal stability and optical bleaching of the 310°C isothermal TL signal in quartz. *Radiation Measurements* **42**, 1285-1293
- Mejdahl, V., Bøtter-Jensen, L., 1994. Luminescence dating of archaeological materials using a new technique based on single aliquot measurements. *Quaternary Geochronology* **13**, 551-554.
- Murray, A.S., Wintle A.G., 2000. Application of the single-aliquot regenerative-dose protocol to the 375°C quartz TL signal. *Radiation Measurements* **32**, 579-583.
- Pagonis, V., Baker, A., Larsen, M., Thompson, Z., 2011. Precision and accuracy of two luminescence dating techniques for retrospective dosimetry: SAR-OSL and SAR-ITL. *Nuclear Instruments and methods in Physics Research B* **269**, 653-663.
- Parkington, J., Rigaud, J.-Ph., Poggenpoel, C., Porraz, G., Texier, P.-J., in prep. Introduction to the project and excavation of Diepkloof Rock Shelter (Western Cape, South Africa): the Middle Stone Age to interrogate. *Journal of Archaeological Science*
- Porraz, G., Miller, C.E., Parkington, J., Rigaud, J.-P., Poggenpoel, C., Tribolo, C., Cartwright, C., Charrié-Duhaut, A., Dayet, L., Goldberg, P., Klein, R.G., Piboule, M., Steele, T., Verna, C., Texier P.-J., in prep. Synthese on the Diepkloof Rock Shelter project. *Journal of Archaeological Science*.
- Richter, D., Krbetschek, M., 2006. A new thermoluminescence dating technique for heated flint. *Archaeometry* **48**, 695-705.
- Richter, D., Temming H., 2006. Testing heated flint palaeodose protocols using dose recovery procedures. *Radiation Measurements* **41**, 819-825.
- Spooner, N.A., Questiaux, D.G., 2000. Kinetics of red, blue and UV thermoluminescence and optically-stimulated luminescence from quartz. *Radiation Measurements* **32**, 659-666.
- Texier P.-J., Porraz G., Parkington J., Rigaud J.-P., Poggenpoel C., Miller C., Tribolo C., Cartwright C., Coudenneau A., Klein R., Steele T., Verna C., 2010. A Howiesons Poort tradition of engraving ostrich eggshell containers dated to 60,000 years ago at Diepkloof Rock Shelter, South Africa, *Proceedings of the National Academy of Science of the United State of America* **107**, 6180-6185.
- Tribolo C., Mercier N., Valladas H., Joron JL, Guibert P., Lefrais Y., M. Selo, Texier P.-J., Rigaud J.-Ph., Porraz G., Poggenpoel C., Parkington J., Texier J.-P., Lenoble A., 2009. Thermoluminescence dating of a Stillbay-Howiesons Poort sequence at Diepkloof Rock Shelter (Western Cape, South Africa). *Journal of Archaeological Science* **36**, 730-739.
- Tribolo, C., Mercier, N., Douville, E., Joron, J.-L., Reyss, J.-L., Rufer, D., Cantin, N., Lefrais, Y., Miller, C.E., Parkington, J., Porraz, G., Rigaud, J.-P., Texier, P.-J., in prep. OSL and TL dating of the Middle Stone Age sequence at Diepkloof Rock Shelter (South Africa): a clarification. *Journal of Archaeological Science*.
- Valladas, H., 1992. Thermoluminescence dating of flint. *Quaternary Science Reviews* **11**, 1-5.
- Vandenbergh, D.A.G., Jain, M., Murray, A. S., 2009. Equivalent dose determination using a quartz isothermal TL signal. *Radiation Measurements* **44**, 439-444.
- Wintle, A.G., 2010. Future directions of luminescence dating of quartz. *Geochronometria* **37**, 1-7.

**Reviewer**  
S. Huot



## Thesis Abstracts

---

**Author:** Ştefan Vasiliniuc  
**Thesis Title:** Luminescence dating of Romanian loess using feldspars  
**Grade:** Ph.D.  
**Date:** October 2011  
**Supervisors:** Constantin Cosma, Alida Timar-Gabor (Babeş-Bolyai University, Cluj Napoca), Peter van den Haute and Dimitri Vandenberghe (Ghent University)  
**Address:** Faculty of Environmental Sciences and Engineering, Babeş-Bolyai University, Fântânele 30, 400294 Cluj Napoca, Romania

Romanian loess-palaeosol sequences are considered semi-continuous and extended archives of climate and environmental change during the Late and Middle Pleistocene. A reliable sedimentation chronology of these deposits would improve our understanding of the regional climatic context and of the link between similar deposits in Europe and Asia. Optically stimulated luminescence (OSL) dating of Romanian loess using quartz has been recently shown to have a significant potential to test the reliability of proxy-based methods and also to provide additional information regarding dust transport and deposition. At the same time, however, OSL dating studies of the loess section near Mircea Vodă (SE Romania) revealed an intriguing dependence of age results on the grain-size fraction of quartz that was used for dating.

This work started by confirming these observations. Single-aliquot regenerative-dose (SAR) OSL dating of silt (4-11µm) and sand-sized (63-90µm) quartz grains extracted from the loess-palaeosol sequence at Mostiştea (SE Romania) yielded ages that are grain-size dependent, indicating that the phenomenon may be characteristic for loess deposits in this region. Detailed investigations into the OSL characteristics did not allow identifying the origin of this discrepancy. The results point at a hitherto unexplained mechanism in OSL production at high doses and question the reliability of obtaining SAR-OSL equivalent doses in the high dose region when a second function is needed to describe the dose response.

The potential for dating of OSL and infrared stimulated luminescence (IRSL) signals from

polymineral silt-sized grains was then investigated. To this purpose, archived material of samples from the loess-palaeosol sequence near Mircea Vodă was used, and all luminescence measurements were made using a SAR protocol.

A double-SAR approach – involving successive stimulation of the polymineral fine grains with IR and blue light, and detection of the resulting IRSL and post-IR OSL signals in the UV – was tested first. Although both signals exhibited significantly different fading rates, the corrected ages are mutually consistent and in agreement with OSL ages for purified silt-sized quartz. This indicates that it may not be necessary to isolate pure quartz to obtain reliable ages for Romanian loess. Owing to the limitations of the fading-correction method, however, the approach is limited to samples from the last glacial period.

A conventional approach, in which stimulation with IR was at 50°C and the detection window in the blue, was also tested. This procedure was not able to provide accurate depositional ages due to initial sensitivity changes induced by preheating at 250°C for 60s and/or contributions from thermally unstable components after less stringent preheat treatments.

Finally, a post-IR IRSL protocol was tested, in which a first stimulation at 50°C was followed by a second stimulation at either 225 or 300°C, and detection was in the blue. Although none of the two post-IR IRSL signals seems to be affected by anomalous fading, only the post-IR IR225 signal yields ages entirely consistent with both OSL ages for silt-sized quartz and independent age control over four interglacial/glacial cycles. The post-IR IR300 signal appears to suffer from dose dependent initial sensitivity changes that hamper its use for the oldest samples investigated.

The results obtained within this work show that silt-sized feldspars can be used to date Romanian loess, thereby providing additional age control for quartz OSL ages. Especially post-IR IR dating of polymineral fine grains is very promising. The obtained age results urge the long-established chronostratigraphical framework for Romanian loess to be revised; the two uppermost well-developed palaeosols can no longer be thought of as interstadial soils that developed during the Last Glacial, but have formed during MIS 5 and MIS 7, respectively.

This thesis is available as a PDF on the Ancient TL web site [www.aber.ac.uk/ancient-tl](http://www.aber.ac.uk/ancient-tl)

**Author :** Georgina King  
**Thesis Title:** Fundamental and sedimentological controls on the luminescence of quartz and feldspar  
**Grade:** Ph.D.  
**Date:** January 2012  
**Supervisors:** Ruth Robinson (St Andrews), Adrian Finch (St Andrews) and David Sanderson (SUERC)  
**Address:** School of Geography and Geosciences, University of St Andrews, Fife, United Kingdom

The optically stimulated luminescence (OSL) characteristics of a suite of quartz and feldspar samples from a range of modern glaciofluvial sediments have been explored to determine the use of OSL as a depositional pathway tracer. Paraglacial and subglacial source material and various glaciofluvial deposits have been analysed from the glacial catchments of Bergsetbreen, Fåbergstølsbreen, and Nigardsbreen as well as the Fåbergstølsgrandane sandur, Jostedal, Norway.

The OSL distribution signatures have been characterised through exploration of sample skewness, kurtosis and overdispersion, and dose distributions of the different depositional settings and source materials are distinct for both quartz and feldspar. Residual ages are greatest for feldspar, indicating significant potential age overestimation where feldspar is used to date glaciofluvial deposits. Sample dose distributions and overdispersion characteristics are driven by source sediment properties, whereas residual ages are controlled by transport and depositional processes. Those transport and depositional processes which result in significant light exposure, also influence dose distributions, and processes that sort sediments least effectively have the highest residual doses.

Sample OSL characteristics, transport distance and grain size distributions have been investigated using factor analysis, as a means of predicting sediment source, facies, depositional process and deposit type. Although the depositional processes of the quartz samples can be clearly differentiated based upon OSL characteristics, factor analyses of feldspar and grain size characteristics are inconclusive.

The application of quartz OSL to the Norwegian samples was limited by its very poor luminescence sensitivity. Quartz is the preferred mineral for OSL, however, despite the plethora of successful quartz OSL applications, the precise origin of the UV/blue luminescence emission, measured during OSL, remains unclear. The origins of this emission and

controls on its intensity were explored using a variety of spectroscopic techniques including photoluminescence, cathodoluminescence, radioluminescence (RL), ionoluminescence (IL) and x-ray excited optical luminescence (XEOL).

Exciting sample luminescence at a range of energies enables exploration of the different donor centres responsible for the luminescence emission. Cathodoluminescence and RL emission spectra are similar, comprising broad emissions at 1.5, 2.0 and 2.7 eV (detection in the UV part of the spectrum was not possible for these experiments). Ionoluminescence emission spectra were dominated by the ~ 3.3 eV emission, which is a component of the signal conventionally monitored during OSL. This emission depleted as a function of dose, to the benefit of the red emission (1.8-2.0 eV) for all samples throughout IL, and similar observations were made for the 3.4 eV emission observed from the XEOL emission spectra. The XEOL spectra are dominated by an emission at ~ 3.8 eV, not widely reported for quartz, which has tentatively been attributed to peroxy linkages. Differences between the IL and XEOL emission spectra are interpreted as evidence for the presence of multiple excited states.

**Author:** Joel Roskin  
**Thesis Title:** The timing and the environmental and palaeoclimatic significance of the late Quaternary dune encroachments into the northwestern Negev Desert, Israel  
**Grade:** Ph.D.  
**Date:** November 2011  
**Supervisors:** Haim Tsoar (Ben-Gurion University of the Negev), Naomi Porat (Geological Survey of Israel) and Dan G. Blumberg (Ben-Gurion University of the Negev)  
**Address:** Department of Geography and Environmental Development, Ben-Gurion University of the Negev, P.O.B. 653, Beer-Sheva, 84105, Israel

This thesis studied the spatial and temporal characteristics of quartz-rich vegetated linear dune (VLD). The time of their encroachments from the northern Sinai Peninsula into the northwestern (NW) Negev desert, subsequent stabilization and the

triggering palaeoclimate, was established by optically stimulated luminescence (OSL) dating.

The dunefield was first divided into geomorphic units that were merged into dune encroachment corridors. Approximately twenty full dune sections at the western and eastern ends of each corridor were analyzed and sampled in outcrops or drills. GPR profiles using a 100-MHz antenna were not found to be a dependable tool for sampling-oriented identification of stratigraphic units.

Ninety-seven samples of aeolian quartz were dated by OSL. Dose recovery tests showed that in the preheat range of 220-280°C, the ratios between measured and given doses is 0.9-0.95. Recycling ratios and preheat plateaus further showed that the sediments are well-suited for the modified single aliquot regenerative-dose (SAR) protocol, that included a thermal cleaning step at the end of each measurement cycle.  $D_e$  distributions were usually normal. Tailing aliquots are attributed to contamination by bioturbation and minute contribution of underlying older sediments. Dose recovery tests showed systematic uncertainties ranging from 2% to 11%, with the greater scatter for the smaller (2 mm) aliquots. These values indicate that samples with  $D_e$  standard deviations lower than ~10% were probably well-bleached at the time of deposition. Disregarding dune crests that have high (>30%) over-dispersion, the age errors usually do not exceed  $\pm 15\%$  and the ages are considered reliable.

Radiocarbon dates on charcoal and ostrich egg shells, and published TL and IRSL ages which were sampled at similar settings, usually agree with the OSL ages, supporting their reliability and significance, and place the entire study area within a single chronological framework.

The OSL ages cluster at ~24-10 ka, ~2-0.8 ka and 150-10 years, matching the chronostratigraphic units of the VLD axis, and representing the major dune mobilization episodes. VLDs accrete sand along their axis during mobilization (elongation) and undergo minute lateral migration. Between mobilization episodes, intermittent local reworking, regulated by strong wintertime storm winds, droughts, and vegetative and biogenic crust cover, resets the luminescence signal of the upper dune sands.

In global terms, the NW Negev dunefield is relatively young. The sand probably originated from the Nile Delta and its availability was limited by the exposure of Delta sands during glacial lower Mediterranean sea-levels. Although sand has been intermittently transported into the Negev for over 100 ka, the dunefield formed only at ~24 ka. Most of the ages cluster at ~16-13.7 ka and at ~12.4-11.6 ka, synchronous with the Heinrich 1 and Younger Dryas cold events, respectively, suggesting a link between global glacial and cold climates to dune mobilization.

The earlier age cluster marks the main encroachment episode that deposited the main bulk of the Negev's sand. At 12.4-11.6 ka, dunes reached the easternmost extent of the dunefield. Based on OSL-dated stratigraphy, the episodes included several rapid incursion events. Encroaching dunes dammed wadis, forming standing-water bodies that supported short-term Epipalaeolithic camp sites.

Calculated dune transport rates that incorporate the range of the OSL age errors are in the range of ~5-25 m/yr. The Negev VLDs encroached in a windier but probably wetter climate than today, providing better conditions for vegetation growth, although when dunes elongated, vegetation was suppressed. It is suggested that the decrease in global windiness between the LGM and the Holocene, as indicated from dust records in ice cores, resulted in global lower-latitude dune stabilization.

The late Holocene (2-0.8 ka) mobilization episode varied from 10 m-thick transverse dune formation to VLD incursion in the western dunefield, and deposited 1-2 m of sand in other parts of the dunefield. Dune erodibility may have resulted from man-induced decimation of vegetation and biogenic crusts. OSL ages, compatible with anthropogenic land-use changes, mark intermittent sand activity and stabilization in the last 150 years, though dune elongation did not ensue.

Sand redness, spectroscopically defined by the redness index (RI) ( $RI=R^2/(B \cdot G^3)$ ), reflecting the amount of iron-oxide quartz-grain coatings, does not vary greatly down the Negev dune sections and across encroachment corridors. RI intensities and the OSL ages of the sand are not correlated and sand grain rubification may have been minimal since deposition or inherited from its Nile source.

The recurring discontinuous aeolian sedimentation pattern found in OSL-dated VLDs provides new and important chronological and sedimentological insight into dune mobilization and stabilization processes, while demonstrating the sensitivity of dunes located along the fringe of the sub-tropical desert belt to climate change and sediment supply. The suggested link between global reductions in cold-climate windiness and low-latitude dune stabilization episodes emphasizes the dominant effect of windiness on major dune mobilizations in low-latitude dunefields even if they are partially vegetated.

This thesis is available as a PDF on the Ancient TL web site [www.aber.ac.uk/ancient-tl](http://www.aber.ac.uk/ancient-tl)

**Author:** Guillaume Guérin  
**Title:** Numerical simulations and modeling of dosimetric effects in Quaternary sediments: application to luminescence dating methods.  
**Grade:** Ph.D.  
**Date:** 19 October 2011  
**Supervisor:** Norbert Mercier  
**Address:** Centre de Recherche en Physique Appliquée à l'Archéologie (CRPAA), Institut de Recherche sur les Archéomatériaux (IRAMAT), UMR 5060, CNRS – Université Michel de Montaigne Bordeaux 3, Maison de l'Archéologie, Esplanade des Antilles, 33607 Pessac Cedex, France.

Luminescence dating methods are based upon the following age equation:

$$\text{Age (a)} = \text{Palaeodose (Gy)} / \text{Dose-rate (Gy.a}^{-1}\text{)}$$

Whereas research on the determination of palaeodose has made significant progress during the last decade, research on dose rates has severely lagged behind. It has long been known that spatial variations in the distribution of radioactivity in sedimentary media at different scales (the range of the different particles/rays involved: alpha, beta, gamma) is limiting the precision and accuracy of luminescence dating methods. However the difficulty in obtaining experimental data has prevented progress in this area of research. In order to resolve this issue, the particle-matter simulation toolkit Geant4 was used in this thesis to study the effects of heterogeneities in sedimentary media.

A series of simulations were designed to refine a field gamma spectrometry technique, with the aim of improving accuracy and precision while reducing measurement times. The results were then used for the experimental calibration of a gamma ray probe. Comparisons between experimental and numerically simulated results of gamma ray spectrometry were very satisfactory and placed the new technique on a secure footing. GEANT4 was then used to define a non-invasive approach, based on surface measurements, which would be adapted to archaeological excavations.

On a grain scale, numerical simulations of dosimetric effects with GEANT4 revealed the limited validity of the widely used concept of infinite matrix in palaeodosimetric dating methods. The initial step

consisted of studying the effect of water on dose rates received by sedimentary grains, an exercise that was conducted in simple geometries. This became the starting point for a review on the use of the infinite matrix assumption and associated concepts. Adequate tools for quantifying a number of identified microdosimetry effects, such as the consequence of radioelement hotspots (e.g. potassium in feldspar grains), were developed and are anticipated to form the basis for a better accuracy in single grain OSL dating methods.

The final part of the thesis focussed upon a chronological study of the Mousterian sequence of Roc de Marsal, which is one of the key sites for the Middle Palaeolithic in South West France. Complex gamma and beta dose rate patterns were identified and their consequences on the ages obtained from heated flints (TL) and quartz samples (OSL) were discussed. The results were then viewed in their palaeoclimatic and palaeoenvironmental context, documented both at a local scale by faunal remains and at a regional scale by pollen studies from a marine sediment core. This chronological study helped placing human occupations on an absolute time scale together with the environment in which the studied Neanderthals were evolving.

The thesis manuscript is partly written in French; however the main results have been published in international journals. As a result, seven chapters consist of papers published in English. This thesis is available as a PDF on the Ancient TL web site [www.aber.ac.uk/ancient-tl](http://www.aber.ac.uk/ancient-tl). Supplementary data is available on request to the author.

## Bibliography

### Compiled by Daniel Richter

---

From 1st November 2011 to 31st May 2012

- Abafoni, J. D., Mallam, S. P., and Akpa, T. C. (2012). Comparison of OSL and ITL measurements on quartz grains extracted from sediments of the Chad Basin, N.E. Nigeria. *Research Journal of Applied Sciences* **6**, 483-486.
- Altay Atlıhan, M., Şahiner, E., and Soykal Alanyalı, F. (2012). Dose estimation and dating of pottery from Turkey. *Radiation Physics and Chemistry* **81**, 594-598.
- Amos, C. B., Lapwood, J. J., Nobes, D. C., Burbank, D. W., Rieser, U., and Wade, A. (2011). Palaeoseismic constraints on Holocene surface ruptures along the Ostler Fault, southern New Zealand. *New Zealand Journal of Geology and Geophysics* **54**, 367-378.
- Andreucci, S., Bateman, M. D., Zucca, C., Kapur, S., Aksit, İ., Dunajko, A., and Pascucci, V. (2012). Evidence of Saharan dust in upper Pleistocene reworked palaeosols of North-west Sardinia, Italy: palaeoenvironmental implications. *Sedimentology* **59**, 917-938.
- Anjar, J., Adrielsson, L., Bennike, O., Björck, S., Filipsson, H. L., Groeneveld, J., Knudsen, K. L., Larsen, N. K., and Möller, P. (2012). Palaeoenvironments in the southern Baltic Sea Basin during Marine Isotope Stage 3: a multi-proxy reconstruction. *Quaternary Science Reviews* **34**, 81-92.
- Athanassas, C., Bassiakos, Y., Wagner, G. A., and Timpson, M. E. (2012). Exploring paleogeographic conditions at two paleolithic sites in Navarino, southwest Greece, dated by optically stimulated luminescence. *Geoarchaeology* **27**, 237-258.
- Atkinson, O. A. C., Thomas, D. S. G., Goudie, A. S., and Parker, A. G. (2012). Holocene development of multiple dune generations in the northeast Rub' al-Khali, United Arab Emirates. *The Holocene* **22**, 179-189.
- Aubry, T., Dimuccio, L. A., Almeida, M., Buylaert, J.-P., Fontana, L., Higham, T., Liard, M., Murray, A. S., Neves, M. J., Peyrouse, J.-B., and Walter, B. (2012). Stratigraphic and technological evidence from the middle palaeolithic-Châtelperronian-Aurignacian record at the Bordes-Fitte rockshelter (Roches d'Abilly site, Central France). *Journal of Human Evolution* **62**, 116-137.
- Bateman, M. D., Bryant, R. G., Foster, I. D. L., Livingstone, I., and Parsons, A. J. (2012). On the formation of sand ramps: A case study from the Mojave Desert. *Geomorphology* **161-162**, 93-109.
- Beerten, K., Deforce, K., and Mallants, D. (2012). Landscape evolution and changes in soil hydraulic properties at the decadal, centennial and millennial scale: A case study from the Campine area, northern Belgium. *Catena* **95**, 73-84.
- Bennett, J. A., Brown, A. G., Schwenninger, J.-L., and Rhodes, E. J. (2011). Holocene channel changes and geoarchaeology of the Exe River, Devon, UK, and the floodplain paradox. In "Geoarchaeology, Climate Change, and Sustainability." (A. G. Brown, L. S. Basell, and K. W. Butzer, Eds.), pp. 135-152. Geological Society of America Special Papers **476**.
- Berner, Z. A., Bleeck-Schmidt, S., Stüben, D., Neumann, T., Fuchs, M., and Lehmann, M. (2012). Floodplain deposits: A geochemical archive of flood history – A case study on the River Rhine, Germany. *Applied Geochemistry* **27**, 543-561.
- Blättermann, M., Frechen, M., Gass, A., Hoelzmann, P., Parzinger, H., and Schütt, B. (2012). Late Holocene landscape reconstruction in the Land of Seven Rivers, Kazakhstan. *Quaternary International* **251**, 42-51.

- Blumer, B. E., Arbogast, A. F., and Forman, S. L. (2012). The OSL chronology of eolian sand deposition in a perched dune field along the northwestern shore of Lower Michigan. *Quaternary Research* **77**, 445-455.
- Bouvier, A., Pinto, G., Guibert, P., Nicolas-Méry, D., and Baylé, M. (2011). Luminescence dating applied to medieval architecture. The north east tower of the Avranches keep (Manche, France). *In "ArchéoSciences."* pp. 59-68.
- Brandes, C., Winsemann, J., Roskosch, J., Meinsen, J., Tanner, D. C., Frechen, M., Steffen, H., and Wu, P. (2012). Activity along the Osning Thrust in Central Europe during the Lateglacial: ice-sheet and lithosphere interactions. *Quaternary Science Reviews* **38**, 49-62.
- Briant, R. M., Kilfeather, A. A., Parfitt, S., Penkman, K. E. H., Preece, R. C., Roe, H. M., Schwenninger, J. L., Wenban-Smith, F. F., and Whittaker, J. E. (2012). Integrated chronological control on an archaeologically significant Pleistocene river terrace sequence: the Thames-Medway, eastern Essex, England. *Proceedings of the Geologists' Association* **123**, 87-108.
- Burbidge, C. I., Richter, D., Sanderson, D. C. W., and Housley, R. A. (2012). Luminescence analyses (OSL and TL) from Karabai I. In "Karabai I. The Palaeolithic Site in Eastern Crimea." (A. Yevtushenko, and V. Chabai, Eds.), pp. 23-34. Archaeological Almanac. Donbass, Donetsk.
- Burrough, S. L., Thomas, D. S. G., Bailey, R. M., and Davies, L. (2012). From landform to process: Morphology and formation of lake-bed barchan dunes, Makgadikgadi, Botswana. *Geomorphology* **161-162**, 1-14.
- Clark, D., Cupper, M., Sandiford, M., and Kiernan, K. (2011). Style and timing of late Quaternary faulting on the Lake Edgar fault, southwest Tasmania, Australia: Implications for hazard assessment in intracratonic areas. *Geological Society of America Special Papers* **479**, 109-131.
- Clemmensen, L. B., Murray, A. S., and Nielsen, L. (2012). Quantitative constraints on the sea-level fall that terminated the Littorina Sea Stage, southern Scandinavia. *Quaternary Science Reviews* **40**, 54-63.
- Cortes A, J., Gonzalez L, G., Binnie, S. A., Robinson, R., Freeman, S. P. H. T., and Vargas E, G. (2012). Paleoseismology of the Mejillones Fault, northern Chile: Insights from cosmogenic Be-10 and optically stimulated luminescence determinations. *Tectonics* **31**, TC2017.
- Costas, S., Jerez, S., Trigo, R. M., Goble, R., and Rebêlo, L. (2012). Sand invasion along the Portuguese coast forced by westerly shifts during cold climate events. *Quaternary Science Reviews* **42**, 15-28.
- Cserkés-Nagy, Á., Thamó-Bozsó, E., Tóth, T., and Sztanó, O. (2012). Reconstruction of a Pleistocene meandering river in East Hungary by VHR seismic images, and its climatic implications. *Geomorphology* **153-154**, 205-218.
- Davidovich, U., Porat, N., Gadot, Y., Avni, Y., and Lipschits, O. (2012). Archaeological investigations and OSL dating of terraces at Ramat Rahel, Israel. *Journal of Field Archaeology* **37**, 192-208.
- Dehnert, A., Lowick, S. E., Preusser, F., Anselmetti, F. S., Drescher-Schneider, R., Graf, H. R., Heller, F., Horstmeyer, H., Kemna, H. A., Nowaczyk, N. R., Züger, A., and Furrer, H. (2012). Evolution of an overdeepened trough in the northern Alpine Foreland at Niederweningen, Switzerland. *Quaternary Science Reviews* **34**, 127-145.
- Demuro, M., Froese, D. G., Arnold, L. J., and Roberts, R. G. (2012). Single-grain OSL dating of glaciofluvial quartz constrains Reid glaciation in NW Canada to MIS 6. *Quaternary Research* **77**, 305-316.
- Derese, C., Vandenbergh, D. A. G., Van Gils, M., Mees, F., Paulissen, E., and Van den haute, P. (2012). Final Palaeolithic settlements of the Campine region (NE Belgium) in their environmental context: Optical age constraints. *Quaternary International* **251**, 7-21.
- Deschodt, L. (2012). Sédimentologie et datation des dépôts fluvio-éoliens du Pléniglaciaire weichselien à Lille (vallée de la Deûle, bassin de l'Escaut, France). *Quaternaire* **23**, 117-127.

- Deschodt, L., Salvador, P.-G., Feray, P., and Schwenninger, J.-L. (2012). Transect partiel de la plaine de la Scarpe (bassin de l'Escaut, nord de la France). Stratigraphie et évolution paléogéographique du Pléniglaciaire supérieur à L'holocène récent. *Quaternaire* **23**, 87-116.
- DeVecchio, D. E., Heermance, R. V., Fuchs, M., and Owen, L. A. (2012). Climate-controlled landscape evolution in the Western Transverse Ranges, California: Insights from Quaternary geochronology of the Saugus Formation and strath terrace flights. *Lithosphere* **4**, 110-130.
- DeVecchio, D. E., Keller, E. A., Fuchs, M., and Owen, L. A. (2012). Late Pleistocene structural evolution of the Camarillo fold belt: Implications for lateral fault growth and seismic hazard in Southern California. *Lithosphere* **4**, 91-109.
- Dörschner, N., Reimann, T., Wenske, D., Lüthgens, C., Tsukamoto, S., Frechen, M., and Böse, M. (2012). Reconstruction of the Holocene coastal development at Fulong Beach in north-eastern Taiwan using optically stimulated luminescence (OSL) dating. *Quaternary International* **263**, 3-13.
- Duller, G. A. T. (2012). Cross-talk during single grain optically stimulated luminescence measurements of quartz and feldspar. *Radiation Measurements* **47**, 219-224.
- Erginal, A. E., Kiyak, N. G., Öztürk, M. Z., Avcioğlu, M., Bozcu, M., and Yiğitbaş, E. (2012). Cementation characteristics and age of beachrocks in a fresh-water environment, Lake İznik, NW Turkey. *Sedimentary Geology* **243-244**, 148-154.
- Fattahi, M., Walker, R. T., Talebian, M., Sloan, R. A., and Rasheedi, A. (2011). The structure and late Quaternary slip rate of the Rafsanjan strike-slip fault, SE Iran. *Geosphere* **7**, 1159-1174.
- Feathers, J. K., Casson, M. A., Schmidt, A. H., and Chithambo, M. L. (2012). Application of pulsed OSL to polymineral fine-grained samples. *Radiation Measurements* **47**, 201-209.
- Fitzsimmons, K. E., Marković, S. B., and Hambach, U. (2012). Pleistocene environmental dynamics recorded in the loess of the middle and lower Danube basin. *Quaternary Science Reviews* **41**, 104-118.
- Fu, X., Zhang, J.-F., and Zhou, L.-P. (2012). Comparison of the properties of various optically stimulated luminescence signals from potassium feldspar. *Radiation Measurements* **47**, 210-218.
- García, A. F., and Mahan, S. A. (2012). The influence of upper-crust lithology on topographic development in the central Coast Ranges of California. *Geomorphology* **138**, 243-262.
- Gartia, R. K., Rey, L., Tejkumar Singh, T., and Basanta Singh, T. (2012). Thermoluminescence of alkali halides and its implications. *Nuclear Instruments and Methods in Physics Research Section B: Beam Interactions with Materials and Atoms* **274**, 129-134.
- Gasparian, P. B. R., Vanhavere, F., and Yukihiro, E. G. (2012). Evaluating the influence of experimental conditions on the photon energy response of Al<sub>2</sub>O<sub>3</sub>:C optically stimulated luminescence detectors. *Radiation Measurements* **47**, 243-249.
- Giunta, G., Gueli, A. M., Monaco, C., Orioli, S., Ristuccia, G. M., Stella, G., and Troja, S. O. (2012). Middle-Late Pleistocene marine terraces and fault activity in the Sant'Agata di Militello coastal area (north-eastern Sicily). *Journal of Geodynamics* **55**, 32-40.
- Gliganic, L. A., Jacobs, Z., Roberts, R. G., Domínguez-Rodrigo, M., and Mabulla, A. Z. P. (2012). New ages for Middle and Later Stone Age deposits at Mumba rockshelter, Tanzania: Optically stimulated luminescence dating of quartz and feldspar grains. *Journal of Human Evolution* **62**, 533-547.
- Guérin, G., and Mercier, N. (2012). Field gamma spectrometry, Monte Carlo simulations and potential of non-invasive measurements. *Geochronometria* **39**, 40-47.

- Guyard, H., St-Onge, G., Pienitz, R., Francus, P., Zolitschka, B., Clarke, G. K. C., Hausmann, S., Salonen, V.-P., Lajeunesse, P., Ledoux, G., and Lamothe, M. (2011). New insights into Late Pleistocene glacial and postglacial history of northernmost Ungava (Canada) from Pingualuit Crater Lake sediments. *Quaternary Science Reviews* **30**, 3892-3907.
- Halfen, A. F., Johnson, W. C., Hanson, P. R., Woodburn, T. L., Young, A. R., and Ludvigson, G. A. (2012). Activation history of the Hutchinson dunes in east-central Kansas, USA during the past 2200 years. *Aeolian Research* **5**, 9-20.
- Harrison, S., Glasser, N. F., Duller, G. A. T., and Jansson, K. N. (2012). Early and mid-Holocene age for the Tempanos moraines, Laguna San Rafael, Patagonian Chile. *Quaternary Science Reviews* **31**, 82-92.
- Harvey, J. E., Pederson, J. L., and Rittenour, T. M. (2011). Exploring relations between arroyo cycles and canyon paleoflood records in Buckskin Wash, Utah: Reconciling scientific paradigms. *Geological Society of America Bulletin* **123**, 2266-2276.
- Homolová, D., Lomax, J., Špaček, P., and Decker, K. (2012). Pleistocene terraces of the Vltava River in the Budějovice basin (Southern Bohemian Massif): New insights into sedimentary history constrained by luminescence data. *Geomorphology* **161–162**, 58-72.
- Huang, C. C., Pang, J., Zha, X., Zhou, Y., Su, H., Wan, H., and Ge, B. (2012). Sedimentary records of extraordinary floods at the ending of the mid-Holocene climatic optimum along the Upper Weihe River, China. *The Holocene* **22**, 675-686.
- Insiripong, S., Kedkaew, C., Thamaphat, K., Chantima, N., Limsuwan, P., and Kaewkhao, J. (2012). Irradiation effect on natural quartz from Zambia. *Procedia Engineering* **32**, 83-89.
- Jacobs, Z., Roberts, R. G., Nespoulet, R., El Hajraoui, M. A., and Debénath, A. (2012). Single-grain OSL chronologies for Middle Palaeolithic deposits at El Mnasra and El Harhoura 2, Morocco: Implications for Late Pleistocene human–environment interactions along the Atlantic coast of northwest Africa. *Journal of Human Evolution* **62**, 377-394.
- Jayangondaperumal, R., Murari, M. K., Sivasubramanian, P., Chandrasekar, N., and Singhvi, A. K. (2012). Luminescence dating of fluvial and coastal red sediments in the SE coast, India, and implications for paleoenvironmental changes and dune reddening. *Quaternary Research* **77**, 468-481.
- Jia, H., Qin, X., and Liu, J. (2012). Environmental changes recorded by major elements in Loulan Stupa section during Early-Middle Holocene. *Journal of Earth Science* **23**, 155-160.
- Kitis, G., Carinou, E., and Askounis, P. (2012). Glow-curve de-convolution analysis of TL glow-curve from constant temperature hot gas TLD readers. *Radiation Measurements* **47**, 258-265.
- Koul, D. K. (2012). Response of pre-dosed TL and OSL emissions of quartz to various stimuli. *Nuclear Instruments and Methods in Physics Research Section B: Beam Interactions with Materials and Atoms* **281**, 82-88.
- Kusiak, J., Lanczont, M., and Bogucki, A. (2012). New exposure of loess deposits in Boyanychi (Ukraine) — Results of thermoluminescence analyses. *Geochronometria* **39**, 84-100.
- Latif, M. B., Fasasi, M. K., and Balogun, F. A. (2012). Low dose TL characteristics of Nigerian fluorite. *Radiation Measurements* **47**, 182-184.
- Lee, S. Y., Seong, Y. B., Shin, Y. K., Choi, K. H., Kang, H. C., and Choi, J. H. (2011). Cosmogenic <sup>10</sup>Be and OSL dating of fluvial strath terraces along the Osip-cheon River, Korea: Tectonic implications. *Geosciences Journal* **15**, 359-378.
- Lepper, K., Gorz, K. L., Fisher, T. G., and Lowell, T. V. (2011). Age determinations for glacial Lake Agassiz shorelines west of Fargo, North Dakota, USA. *Canadian Journal of Earth Sciences* **48**, 1199-1207.

- Li, B., and Li, S.-H. (2012). A reply to the comments by Thomsen et al. on "Luminescence dating of K-feldspar from sediments: A protocol without anomalous fading correction". *Quaternary Geochronology* **8**, 49-51.
- Li, B., Li, S.-H., and Sun, J. (2011). Isochron dating of sand-loess-soil deposits from the Mu Us Desert margin, central China. *Quaternary Geochronology* **6**, 556-563.
- Li, S.-H., and Fan, A. (2011). OSL chronology of sand deposits and climate change of last 18 ka in Gurbantunggut Desert, northwest China. *Journal of Quaternary Science* **26**, 813-818.
- Li, S.-H., Sun, J., and Li, B. (2012). Holocene environmental changes in central Inner Mongolia revealed by luminescence dating of sediments from the Sala Us River valley. *The Holocene* **22**, 397-404.
- Liu, K., and Lai, Z. P. (2012). Chronology of Holocene sediments from the archaeological Salawusu site in the Mu Us Desert in China and its palaeoenvironmental implications. *Journal of Asian Earth Sciences* **45**, 247-255.
- Long, H., Lai, Z., Fuchs, M., Zhang, J., and Yang, L. (2012). Palaeodunes intercalated in loess strata from the western Chinese Loess Plateau: Timing and palaeoclimatic implications. *Quaternary International* **263**, 37-45.
- Loope, W. L., Loope, H. M., Goble, R. J., Fisher, T. G., Lytle, D. E., Legg, R. J., Wysocki, D. A., Hanson, P. R., and Young, A. R. (2012). Drought drove forest decline and dune building in eastern upper Michigan, USA, as the upper Great Lakes became closed basins. *Geology* **40**, 315-318.
- Lowick, S. E., Trauerstein, M., and Preusser, F. (2012). Testing the application of post IR-IRSL dating to fine grain waterlain sediments. *Quaternary Geochronology* **8**, 33-40.
- Lukas, S., Preusser, F., Anselmetti, F. S., and Tinner, W. (2012). Testing the potential of luminescence dating of high-alpine lake sediments. *Quaternary Geochronology* **8**, 23-32.
- Lüthgens, C., and Böse, M. (2011). Chronology of Weichselian main ice marginal positions in north-eastern Germany. *E&G Quaternary Science Journal* **60**, 236-247.
- Mason, J. A., Swinehart, J. B., Hanson, P. R., Loope, D. B., Goble, R. J., Miao, X., and Schmeisser, R. L. (2011). Late Pleistocene dune activity in the central Great Plains, USA. *Quaternary Science Reviews* **30**, 3858-3870.
- McCalpin, J. P., Harrison, J. B. J., Berger, G. W., and Tobin, H. C. (2011). Paleoseismicity of a low-slip-rate normal fault in the Rio Grande rift, USA: The Calabacillas fault, Albuquerque, New Mexico. *Geological Society of America Special Papers* **479**, 23-46.
- Medialdea, A., Porat, N., and Benito, G. (2011). Optically stimulated luminescence characteristics of modern flash-flood deposits in small mountain catchments. *Spectroscopy Letters* **44**, 530-534.
- Mehta, M., Majeed, Z., Dobhal, D., and Srivastava, P. (2012). Geomorphological evidences of post-LGM glacial advancements in the Himalaya: A study from Chorabari Glacier, Garhwal Himalaya, India. *Journal of Earth System Science* **121**, 149-163.
- Muñoz-Salinas, E., Bishop, P., Zamorano, J.-J., and Sanderson, D. (2012). Sedimentological processes in lahars: Insights from optically stimulated luminescence analysis. *Geomorphology* **136**, 106-113.
- Nair, R., Murari, M., Lakshmi, C., Buynevich, I., Goble, R., Srinivasan, P., Murthy, S., Trivedi, D., Kandpal, S., Hussain, S., Sengupta, D., and Singhvi, A.K. Subsurface signatures and timing of extreme wave events along the southeast Indian coast. *Journal of Earth System Science*, **120**, 873-883.
- Neves, W. A., Araujo, A. G. M., Bernardo, D. V., Kipnis, R., and Feathers, J. K. (2012). Rock Art at the Pleistocene/Holocene Boundary in Eastern South America. *Plos One* **7**, e32228.

- Olig, S. S., Eppes, M. C., Forman, S. L., Love, D. W., and Allen, B. D. (2011). Late Quaternary earthquakes on the Hubbell Spring fault system, New Mexico, USA: Evidence for noncharacteristic ruptures of intrabasin faults in the Rio Grande rift. *Geological Society of America Special Papers* **479**, 47-77.
- Oniya, E. O., Polymeris, G. S., Tsirliganis, N. C., and Kitis, G. (2012). Radiation dose response correlation between thermoluminescence and optically stimulated luminescence in quartz. *Journal of Luminescence* **132**, 1720-1728.
- Pagonis, V., Chen, R., and Lawless, J. L. (2012). Superlinear dose response of thermoluminescence (TL) and optically stimulated luminescence (OSL) signals in luminescence materials: An analytical approach. *Journal of Luminescence* **132**, 1446-1455.
- Pelletier, J. D., Quade, J., Goble, R. J., and Aldenderfer, M. S. (2011). Widespread hillslope gullying on the southeastern Tibetan Plateau: Human or climate-change induced? *Geological Society of America Bulletin* **123**, 1926-1938.
- Pigati, J. S., Miller, D. M., Bright, J. E., Mahan, S. A., Nekola, J. C., and Paces, J. B. (2011). Chronology, sedimentology, and microfauna of groundwater discharge deposits in the central Mojave Desert, Valley Wells, California. *Geological Society of America Bulletin* **123**, 2224-2239.
- Polymeris, G. S., and Kitis, G. (2011). IRSL dating of a deep water core from Pylos, Greece; comparison to post IR blue OSL and TL dating results. *Mediterranean Archaeology and Archaeometry* **11**, 107-120.
- Polymeris, G. S., Oniya, E. O., Jibiri, N. N., Tsirliganis, N. C., and Kitis, G. (2012). In-homogeneity in the pre-dose sensitization of the 110 degrees C TL peak in various quartz samples: The influence of annealing. *Nuclear Instruments & Methods in Physics Research Section B-Beam Interactions with Materials and Atoms* **274**, 105-110.
- Prendergast, A. L., Cupper, M. L., Jankaew, K., and Sawai, Y. (2012). Indian Ocean tsunami recurrence from optical dating of tsunami sand sheets in Thailand. *Marine Geology* **295-298**, 20-27.
- Preusser, F., Rufer, D., and Schreurs, G. (2011). Direct dating of Quaternary phreatic maar eruptions by luminescence methods. *Geology* **39**, 1135-1138.
- Qin, X., Liu, J., Jia, H., Lu, H., Xia, X., Zhou, L., Mu, G., Xu, Q., and Jiao, Y. (2012). New evidence of agricultural activity and environmental change associated with the ancient Loulan kingdom, China, around 1500 years ago. *The Holocene* **22**, 53-61.
- Rasse, M., Tribolo, C., Soriano, S., and Huysecom, E. (2012). Premières données chronostratigraphiques sur les formations du Pléistocène supérieur de la « falaise » de Bandiagara (Mali, Afrique de l'Ouest). *Quaternaire* **23**, 5-23.
- Raukas, A., and Stankowski, W. (2011). On the age of the Kaali craters, Island of Saaremaa, Estonia. *Baltica* **24**, 37-44.
- Richter, D., Moser, J., and Nami, M. (2012). New data from the site of Ifri n'Ammar (Morocco) and some remarks on the chronometric status of the Middle Paleolithic in the Maghreb. In "Modern Origins: A North African Perspective." (J.-J. Hublin, and S. McPherron, Eds.), pp. 61-78. Vertebrate Paleobiology and Paleoanthropology. Springer, Dordrecht.
- Rose, J. I., Usik, V. I., Marks, A. E., Hilbert, Y. H., Galletti, C. S., Parton, A., Geiling, J. M., Černý, V., Morley, M. W., and Roberts, R. G. (2011). The Nubian Complex of Dhofar, Oman: An African Middle Stone Age Industry in Southern Arabia. *PLoS ONE* **6**, e28239.
- Rosenberg, T. M., Preusser, F., Blechschmidt, I., Fleitmann, D., Jagher, R., and Matter, A. (2012). Late Pleistocene palaeolake in the interior of Oman: a potential key area for the dispersal of anatomically modern humans out-of-Africa? *Journal of Quaternary Science* **27**, 13-16.

- Rosenberg, T. M., Preusser, F., Fleitmann, D., Schwalb, A., Penkman, K., Schmid, T. W., Al-Shanti, M. A., Kadi, K., and Matter, A. (2011). Humid periods in southern Arabia: Windows of opportunity for modern human dispersal. *Geology* **39**, 1115-1118.
- Roskin, J., Blumberg, D. G., Porat, N., Tsoar, H., and Rozenstein, O. (2012). Do dune sands redden with age? The case of the northwestern Negev dunefield, Israel. *Aeolian Research* **5**, 63-75.
- Rowan, A. V., Roberts, H. M., Jones, M. A., Duller, G. A. T., Covey-Crump, S. J., and Brocklehurst, S. H. (2012). Optically stimulated luminescence dating of glaciofluvial sediments on the Canterbury Plains, South Island, New Zealand. *Quaternary Geochronology* **8**, 10-22.
- Rufer, D., Gnos, E., Mettler, R., Preusser, F., and Schreurs, G. (2012). Proposing new approaches for dating young volcanic eruptions by luminescence methods. *Geochronometria* **39**, 48-56.
- Sanjurjo-Sánchez, J., and Vidal Romani, J. R. (2011). Luminescence dating of pseudokarst speleothems: A first approach. *Spectroscopy Letters* **44**, 543-548.
- Schmidt, S., Tsukamoto, S., Salomon, E., Frechen, M., and Hetzel, R. (2012). Optical dating of alluvial deposits at the orogenic front of the andean precordillera (Mendoza, Argentina). *Geochronometria* **39**, 62-75.
- Sohbati, R., Murray, A. S., Buylaert, J.-P., Ortuño, M., Cunha, P. P., and Masana, E. (2012). Luminescence dating of Pleistocene alluvial sediments affected by the Alhama de Murcia fault (eastern Betics, Spain) – a comparison between OSL, IRSL and post-IR IRSL ages. *Boreas* **41**, 250-262.
- Soni, A., Mishra, D. R., Bhatt, B. C., Gupta, S. K., Rawat, N. S., Kulkarni, M. S., and Sharma, D. N. (2012). Characterization of deep energy level defects in  $\alpha$ -Al<sub>2</sub>O<sub>3</sub>:C using thermally assisted OSL. *Radiation Measurements* **47**, 111-120.
- Srinivasa Sarma, C., and Rama Reddy, K. (2012). The effect of ultrasonic perturbation on F-centers in KCl: A thermoluminescence study. *Radiation Measurements* **47**, 191-194.
- Srivastava, P., and Misra, D. K. (2012). Optically stimulated luminescence chronology of terrace sediments of Siang River, Higher NE Himalaya: comparison of quartz and feldspar chronometers. *Journal of the Geological Society of India* **79**, 252-258.
- Stolz, C., Grunert, J., and Fülling, A. (2012). The formation of alluvial fans and young floodplain deposits in the Lieser catchment, Eifel Mountains, western German Uplands: A study of soil erosion budgeting. *The Holocene* **22**, 267-280.
- Subedi, B., Polymeris, G. S., Tsirliganis, N. C., Pagonis, V., and Kitis, G. (2012). Reconstruction of thermally quenched glow curves in quartz. *Radiation Measurements* **47**, 250-257.
- Suchodoletz, H. v., Blanchard, H., Hilgers, A., Radtke, U., Fuchs, M., Dietze, M., and Zöller, L. (2012). TL and ESR dating of Middle Pleistocene lava flows on Lanzarote island, Canary Islands (Spain). *Quaternary Geochronology* **9**, 54-64.
- Sugisaki, S., Buylaert, J. P., Murray, A. S., Harada, N., Kimoto, K., Okazaki, Y., Sakamoto, T., Iijima, K., Tsukamoto, S., Miura, H., and Nogi, Y. (2012). High resolution optically stimulated luminescence dating of a sediment core from the southwestern Sea of Okhotsk. *Geochemistry Geophysics Geosystems* **13**, Q0AA22.
- Sun, Y., Clemens, S. C., Morrill, C., Lin, X., Wang, X., and An, Z. (2012). Influence of Atlantic meridional overturning circulation on the East Asian winter monsoon. *Nature Geoscience* **5**, 46-49.
- Tamura, T., Saito, Y., Nguyen, V. L., Ta, T. K. O., Bateman, M. D., Matsumoto, D., and Yamashita, S. (2012). Origin and evolution of intertributary delta plains; insights from Mekong River delta. *Geology* **40**, 303-306.

Telfer, M. W., Thomas, Z. A., and Breman, E. (2012). Sand ramps in the Golden Gate Highlands National Park, South Africa: Evidence of periglacial aeolian activity during the last glacial. *Palaeogeography, Palaeoclimatology, Palaeoecology* **313–314**, 59-69.

Thomsen, K. J., Murray, A., Jain, M., and Buylaert, J.-P. (2012). Re 'Luminescence dating of K-feldspar from sediments: a protocol without anomalous fading correction' by Bo Li and Sheng-Hua Li. *Quaternary Geochronology* **8**, 46-48.

Timar-Gabor, A., Vasiliniuc, S., Vandenberghe, D. A. G., Constantin, D., and Cosma, C. (2011). Luminescence dating of archaeological materials and sediments in Romania using quartz. *Romanian Reports on Physics* **63**, 929-939.

Topaksu, M., Correcher, V., Garcia-Guinea, J., Topak, Y., and Göksu, H. Y. (2012). Comparison of thermoluminescence (TL) and cathodoluminescence (ESEM-CL) properties between hydrothermal and metamorphic quartzes. *Applied Radiation and Isotopes* **70**, 946-951.

Vojtko, R., Marko, F., Preusser, F., Madarás, J., and Kováčová, M. (2011). Late quaternary fault activity in the western Carpathians: Evidence from the vikartovce fault (Slovakia). *Geologica Carpathica* **62**, 563-574.

Wang, X., Chai, C., Du, P., Lei, Q., Yin, G., and Lu, Y. (2012). Luminescence age constraints on palaeo-earthquake events along the lingwu fault in the Yinchuan Basin, China. *Geochronometria* **39**, 57-61.

Wang, X. L., and Wintle, A. G. (2012). Optically stimulated luminescence production in the single-aliquot regenerative dose protocol. *Radiation Measurements* **47**, 121-129.

Wang, X. L., Wintle, A. G., and Adamiec, G. (2012). Improving the reliability of single-aliquot regenerative dose dating using a new method of data analysis. *Quaternary Geochronology* **9**, 65-74.

Wenske, D., Frechen, M., Böse, M., Reimann, T., Tseng, C.-H., and Hoelzmann, P. (2012). Late Quaternary river terraces in the Central Mountain Range of Taiwan: A study of cover sediments across a terrace section along the Tachia River. *Quaternary International* **263**, 26-36.

Wilkins, D., De Deckker, P., Fifield, L. K., Gouramanis, C., and Olley, J. (2012). Comparative optical and radiocarbon dating of laminated Holocene sediments in two maar lakes: Lake Keilambete and Lake Gnotuk, south-western Victoria, Australia. *Quaternary Geochronology* **9**, 3-15.

Yi, L., Yu, H.-J., Ortiz, J. D., Xu, X.-Y., Chen, S.-L., Ge, J.-Y., Hao, Q.-Z., Yao, J., Shi, X.-F., and Peng, S.-Z. (2012). Late Quaternary linkage of sedimentary records to three astronomical rhythms and the Asian monsoon, inferred from a coastal borehole in the south Bohai Sea, China. *Palaeogeography, Palaeoclimatology, Palaeoecology* **329–330**, 101-117.

Yu, L., and Lai, Z. (2012). OSL chronology and palaeoclimatic implications of aeolian sediments in the eastern Qaidam Basin of the northeastern Qinghai-Tibetan Plateau. *Palaeogeography, Palaeoclimatology, Palaeoecology* **337–338**, 120-129.

Yuan, D.-Y., Champagnac, J.-D., Ge, W.-P., Molnar, P., Zhang, P.-Z., Zheng, W.-J., Zhang, H.-P., and Liu, X.-W. (2011). Late Quaternary right-lateral slip rates of faults adjacent to the lake Qinghai, northeastern margin of the Tibetan Plateau. *Geological Society of America Bulletin* **123**, 2016-2030.

Zhang, J., Jia, Y., Lai, Z., Long, H., and Yang, L. (2011). Holocene evolution of Huangqihai Lake in semi-arid northern China based on sedimentology and luminescence dating. *The Holocene* **21**, 1261-1268.

Zhao, H., Li, G., Sheng, Y., Jin, M., and Chen, F. (2012). Early–middle Holocene lake-desert evolution in northern Ulan Buh Desert, China. *Palaeogeography, Palaeoclimatology, Palaeoecology* **331–332**, 31-38.

Zink, A. J. C., Susino, G. J., Porto, E., and Huffman, T. N. (2012). Direct OSL dating of Iron Age pottery from South Africa – Preliminary dosimetry investigations. *Quaternary Geochronology* **8**, 1-9.

## Conference Announcements

---



### UK Luminescence and ESR meeting

12<sup>th</sup>-14<sup>th</sup> September 2012

The next UK luminescence and ESR dating research meeting will be held at Aberystwyth University from the 12-14th September 2012. The meeting is intended to provide a forum for the presentation and discussion of the latest research in luminescence and ESR dating and related work. Presentations covering basic physics, methodological issues and the application of these techniques are all welcome. The meeting will consist of both oral and poster presentations, and presentations by research students are particularly encouraged.

The second circular contains information about the deadlines for submitting abstracts, booking accommodation, and registration. It also contains the relevant forms for registering for the conference, securing accommodation on the University Campus, and for making payment. The circular is available from the conference web site :

[www.aber.ac.uk/en/iges/research-groups/quaternaly/luminescence-research-laboratory/uklum2012/](http://www.aber.ac.uk/en/iges/research-groups/quaternaly/luminescence-research-laboratory/uklum2012/)

#### **Conference deadlines**

1. Abstract submission  
- 17th July 2012
2. Payment of registration and accommodation  
- 27th July 2012

Professor Geoff Duller  
Dr Helen Roberts

Institute of Geography and Earth Sciences,  
Aberystwyth University,  
Ceredigion, SY23 3DB,  
United Kingdom  
E-mail: [uklum2012@aber.ac.uk](mailto:uklum2012@aber.ac.uk)



# Submission of articles to Ancient TL

---

## Reviewing System

In order to ensure acceptable standards and minimize delay in publication, a modification of the conventional refereeing system has been devised for Ancient TL:

Articles can be sent directly by authors to a member of the Reviewers Panel chosen on the basis of the subject matter, but who is not in any of the authors' laboratories. **At the discretion of the Editor**, reviewers who are not listed in the Panel may be used.

The reviewing system aims to encourage direct dialogue between author and reviewer. The Editor should be kept advised of the progress of articles under review by sending him copies of all correspondence. He is available for advice where reviewing difficulties have arisen. Authors whose mother tongue is not English are required to have their manuscript revised for English *before* submitting it.

We ask reviewers to specify (where required) the minimum of revision that is consistent with achieving a clear explanation of the subject of the paper, the emphasis being on *rapid* publication; reviewers are encouraged to make a brief written comment for publication at the end of the paper. Where a contribution is judged not to meet an adequate standard without substantial modification, the author will be advised that the contribution is not suitable for publication. Articles that are not considered to be of sufficient interest may also be rejected.

## Procedures

1. Articles should be submitted to an appropriate member of the Reviewing Panel or Editorial Board, chosen on the basis of the subject matter, but who is not in any of the authors' laboratories.
2. Articles should not normally exceed the equivalent of 5000 words inclusive of diagrams, tables and references. Greater space will be appropriate for certain topics; for these the Editor should first be consulted.  
Short notes and letters are also invited. These should not exceed two printed pages in Ancient TL, including diagrams, tables and references (equivalent to ~1400 words of text).
3. Diagrams and labels should be ready for direct reproduction and not normally exceed 12 cm wide by 10 cm high. Where possible, high quality electronic versions of figures should be submitted. Separate figure captions should be supplied. Inappropriately scaled drawings and labels will be returned for alteration.
4. Authors are asked to submit the paper, including diagrams, to the Reviewer and a duplicate copy to the Editor.  
The final version of the text must be submitted to the Editor electronically using a standard format (Microsoft Word for PC is currently used for producing Ancient TL). Electronic copies of Diagrams and Tables should also be submitted.
5. Upon receipt of an article, the Editor will send an acknowledgement to the author. If the Reviewer is unable to deal with the contribution within **4 weeks** he/she will inform the author and advise the Editor.

## Requirements under various situations

*When agreement concerning an article has been reached:*

The Editor should receive a copy of the final version of the paper, both as hard copy and electronically. The Reviewer should send their final decision, including comments for publication if any, to the Editor.

*If the article has not been rejected, but agreement on its final form cannot be reached or where there are protracted delays in the reviewing process:*

The Editor may request an assessment from the Reviewer and responsibility passes to the Editor.

*If the article is rejected:*

The Editor and author receive notification from the Reviewer, with an indication of the reason for rejection.

**Thesis abstracts** are to be sent to the Editor and in principle do not need reviewing. However, authors are requested to make sure that the English is correct before submission. Thesis abstracts should not exceed 750 words, and figures and tables are not accepted.

**Advertising.** Formal information on equipment can be published in Ancient TL. It should not exceed one printed page. Current charges are displayed on the website (<http://www.aber.ac.uk/ancient-tl>)

## Subscriptions to Ancient TL

Ancient TL is published 2 times a year and is sent Airmail to subscribers outside the United Kingdom. While every attempt will be made to keep to publication schedule, the Editorial Board may need to alter the number and frequency of issues, depending on the number of available articles which have been accepted by reviewers.

The subscription rate for 2012 is £15 for individual subscribers and £25 for Institutional subscription, plus any taxes where required. Payment must be in pounds sterling. Enquiries and orders must be sent to the Editor. Payment may be by cheques, made payable to 'Aberystwyth University', by credit/debit cards or by bank transfers. Further information on subscriptions is available on the Ancient TL web site (<http://www.aber.ac.uk/ancient-tl>)